THESIS

This is to certify that the

dissertation entitled
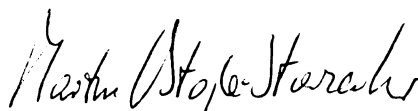
PLASTICITY OF RANDOM MEDIA

presented by

Horea Tiberiu Ilies

has been accepted towards fulfillment
of the requirements for

__Master's__ degree in __Mechanics__

Major professor

Date __May 18, 1995__

**LIBRARY
Michigan State
University**

DATE DUE	DATE DUE	DATE DUE
————————	————————	————————
————————	————————	————————
————————	————————	————————
————————	————————	————————
————————	————————	————————
————————	————————	————————
————————	————————	————————

PLASTICITY OF RANDOM MEDIA

by

Horea Tiberiu Ilies

A THESIS

Submitted to
Michigan State University
in partial fulfillment of the requirements
for the degree of

MASTER OF SCIENCE

Department of Materials Science and Mechanics

1995.

ABSTRACT

PLASTICITY OF RANDOM MEDIA

by

Horea Tiberiu Ilies

Effects of spatial random fluctuations in the yield condition are analyzed in rigid-perfectly plastic media governed, generally, by a Huber-Mises-Henky or Mohr-Coulomb yield condition with cohesion. A weakly random plastic microstructure is modelled, on a continuum mesoscale, by an isotropic yield condition with the yield limit taken as a locally averaged random field. The solution method is based on a stochastic generalization of the method of slip-lines, whose significant feature is that the deterministic characteristics are replaced by the forward evolution cones containing random characteristics. For the Huber-Mises-Henky medium, an application of the method is given to the limit analysis of a cylindrical tube under internal traction. For the Mohr-Coulomb medium, the characteristic boundary value problem is studied, with an emphasis on variation of the statistical characteristics of the field variables at the extremum point considering both uniform and Weibull type random variates. The major conclusion is that weak material randomness always leads to a relatively stronger scatter in the position and field variables as well as to a larger size of the domain of dependence - effects which are amplified by both, grown noise and inhomogeneity in the boundary data.

ACKNOWLEDGEMENT

TABLE OF CONTENTS

1. INTRODUCTION

Today we are experiencing a revolution in materials used in a broad variety of engineering applications; incremental improvements in traditional materials will not do the job! In the course of history, major shifts to new types of materials were always accompanied by significant design changes that better used the potential of these new materials. Mechanicians are creating new models that aim to better describe the behavior of real materials. Among various effects that need to be accounted for is randomness, which may, generally, be due to:

- random external loading

- random boundary conditions and data

- randomness in physical behavior of engineering materials due to fluctuations in their parameters and properties.

In this work we investigate the effects of random spatial fluctuations in the yield function of random rigid perfectly-plastic media. In [Olszak et al, 1962] was mentioned the subject of plasticity of randomly inhomogeneous media. This important reference provides, among others, a very good review and discussion of the methods used to solve boundary value problems of plasticity of inhomogeneous media described by deterministic functions which, in principle, form the starting point for stochastic problems. These methods are: analytical, approximate, inverse and semi-inverse, respectively. Given the power of today's computers on one hand and the limitations of analytical and inverse solutions in deterministic non-homogeneous medium problems on the other, we adopt a com-

putational method to solve the system of quasi-linear hyperbolic differential equations that governs the problem. The solution is based on a stochastic generalization of the method of slip-lines, whose significant feature is that it replaces the deterministic characteristics by cones of forward evolution.

Plasticity of randomly inhomogeneous media has recently been studied by [Nordgren, 1992] from a different standpoint. The focus there has been on a stochastic formulation of lower-bound and upper-bound theorems and a corresponding application to the loading of a wedge. While we postpone the discussion of relative merits of Nordgren's and our approaches to Chapter 4, the principal difference between them is the recognition, in our model, of the scale-dependence of a Representative Volume Element of a random continuum approximation (see Section 1.1 below).

The method used in this work applies to media that require a stochastic continuum formulation, i.e. when the fluctuations in constitutive laws disappear only at scales larger than the macroscopic dimension of the body [Ostoja-Starzewski, 1992a].

A generalization of the method of characteristics extended to the flow of rigid perfectly plastic and spatially random media has been developed in [Ostoja-Starzewski, 1992a], where a comparison of solutions of a specific Cauchy problem in the case of a deterministic homogeneous medium with the yield limit k_{det} and a random medium case having the same average yield limit $\langle k \rangle = k_{det}$ and a weak random noise was illustrated. It was found that such a weak material randomness has strong effects in the case of

inhomogeneous boundary value data. The influence of these random fluctuations upon the Cauchy and Characteristic boundary value problems for media whose plastic behavior can be approximated by the isotropic form:

$$(\sigma_x - \sigma_y)^2 + 4\tau_{xy}^2 = 4k_\delta^2(\omega) \tag{1.1}$$

was examined in [Ostoja-Starzewski, 1992a, 1992b] and it was found that a weak material randomness always leads to a relatively much stronger scatter in the position and field variables and that there is practically no difference in the slip-line nets given by the integration method (i.e. explicit or implicit). Moreover, in [Ostoja-Starzewski, and Ilies, 1995] a practical problem was solved, namely a tube made of a random rigid perfectly plastic medium under internal load, whose yield function may be approximated by (1.1); the paper summarizes the findings presented in detail in the following chapter. There it was found that, even though the scatter in the slip-line nets increase with the inhomogeneity of data on the boundary as well as with the random noise, the average solution of the stochastic problem is basically the same as the solution of the homogeneous medium problem

In the case of granular materials, the medium's response is usually approximated by an isotropic Mohr-Coulomb yield criterion:

$$\frac{1}{4}(\sigma_x - \sigma_y)^2 + \tau_{xy}^2 = \frac{(\sin\rho_\delta)^2}{4}(\sigma_x + \sigma_y + 2H_\delta)^2 \tag{1.2}$$

in which ρ_δ and H_δ are random variables.

The Mohr-Coulomb yield criterion (1.2) is expected to give a highly nonlinear behavior. The slip-line theory for the deterministic homogeneous granular media was developed in [Sokolowskii, 1965], but the effect of the random spatial fluctuations upon the medium's behavior was not yet studied. In this case we apply the same computational method of solving the system of governing quasi-linear hyperbolic differential equations as in the case of media whose yield function can be approximated by (1.1). This is studied in chapter 3.

In micromechanics of granular media, randomness is typically accounted for by either solving a set of deterministic boundary value problems of large system of disks (one obstacle being in this case the computer limitations on the sizes of large lattices representing discrete media), or by solving a single boundary value problem for a medium that has average properties, case in which there arise difficulties in finding the correct average of the random properties such that the two solutions coincide.

1.1 Random Continuum Plastic Medium.

By a *random microstructure* (or *medium*) we understand a family:

$$\mathbf{B} = \{\mathbf{B}(\omega), \omega \in \Omega\} \tag{1.3}$$

of deterministic media $\mathbf{B}(\omega)$, where ω is an index for the probability space Ω. A paradigm of derivation of a stochastic continuum model is presented in [Ostoja-Starzewski,

1992a]. This relies on the concept of a *window* bounding a random microstructure:

$$\mathbf{B}_\delta = \{\mathbf{B}_\delta(\omega), \omega \in \Omega\} \tag{1.4}$$

where $\mathbf{B}_\delta(\omega)$ is a single realization and $\delta = \dfrac{L}{d}$ is a non-dimensional scale parameter that characterizes the scale L of observation relative to a typical microscale d of the material structure. Therefore, the window may be interpreted as a Representative Volume Element (RVE) of an approximating random continuum $\mathbf{B}_\delta$. The effective properties display a statistical scatter which decreases to 0 as $\delta \to \infty$. While there exists a finite scale δ at which this scatter may be considered negligible, such an approach does not apply in situations where δ is comparable to, or greater than, the macroscopic (relative) dimension δ_M of the body B. In this case the stochastic formulation of a given boundary value problem is needed. In [Ostoja-Starzewski, 1992a] six steps for determination of a random rigid perfectly-plastic medium are outlined.

2. PLASTICITY OF METALS

2.1 Continuum Field Equations

The state of plastic plane flow, whose generalization to materials governed by random yield functions (i.e. (1.1) and (1.2)) is studied in this work, is defined by the fundamental property that the displacements of all particles of the body are parallel to a given plane, usually chosen to be xOy of the rectangular, or Cartesian, system of coordinates xOyz. The displacements are considered to be independent of z coordinate. Therefore, each point of the continuum will be characterized by four stress components σ_x, σ_y, τ_{xy} in the xOy plane and σ_z parallel to Oz axis. Since under the initial assumption of plane flow, the tangential components $\tau_{xz}=\tau_{yz}=0$, σ_z is found to be a principal stress.

Another assumption that is made is that the material can be approximated by a rigid perfectly-plastic medium, see Fig 2.1:
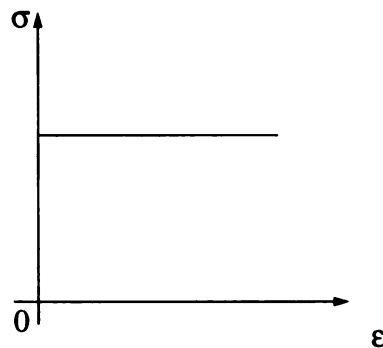

Fig 2.1 The rigid-perfectly plastic medium

It is noted at this stage that the elastic part of deformation and the strain hardening effects

6

are being disregarded in the present model, although the strain hardening can be introduced later. Furthermore, we will neglect the inertia terms in the field equations because at this time, a general solution of problems of plane flow accounting for inertia terms is not available. We can neglect these inertia terms on the consideration that in most material forming processes and practical problems, accelerations of the material are very small, therefore the influence of inertia forces is negligible. An estimation of the influence of inertial forces can be found in [Szczepinski, 1979, ch. 6].

With the above assumptions, the equilibrium equations of the field reduce to the well known form:

$$\frac{\partial \sigma_x}{\partial x} + \frac{\partial \tau_{xy}}{\partial y} = 0 \tag{2.1}$$

$$\frac{\partial \sigma_y}{\partial y} + \frac{\partial \tau_{xy}}{\partial x} = 0 \tag{2.2}$$

The random yield function:

$$F_\delta(\omega) = 0 \tag{2.3}$$

is approximated by an isotropic form (Von Mises):

$$(\sigma_x - \sigma_y)^2 + 4\tau_{xy}^2 = 4k_\delta^2(\omega) \tag{2.4}$$

where the yield limit $k_\delta(\omega)$, at any point $\underline{x}$, is a random variable that can be considered as a sum of the mean and a random fluctuation:

$$k_\delta(\underline{x}, \omega) = \langle k_\delta(\underline{x}, \omega) \rangle + k_\delta'(\underline{x}, \omega), \quad \langle k_\delta'(\underline{x}, \omega) \rangle = 0 \qquad (2.5)$$

Clearly, $k_\delta(\underline{x}, \omega)$ and $k_\delta'(\underline{x}, \omega)$ are random fields.

At this point, in the theory of slip-lines [Chakrabarty, 1987, Szczepinski, 1979], two new functions p and φ are introduced:

$$\sigma_x = p + k_\delta \cos(2\varphi) \qquad (2.6)$$

$$\sigma_y = p - k_\delta \cos(2\varphi) \qquad (2.7)$$

$$\tau_{xy} = k_\delta \sin(2\varphi) \qquad (2.8)$$

These expressions satisfy identically the yield function (2.4). Substituting (2.6), (2.7) and (2.8) in the field equations (2.1) and (2.2) and setting $\varphi = -\dfrac{\pi}{4}$, one obtains a basic set of partial differential equations in two unknowns, p and φ:

$$\frac{\partial p}{\partial x} + 2k_\delta \frac{\partial \varphi}{\partial x} = \frac{\partial k_\delta}{\partial y} \qquad (2.9)$$

$$\frac{\partial p}{\partial y} - 2k_\delta \frac{\partial \varphi}{\partial y} = \frac{\partial k_\delta}{\partial x} \qquad (2.10)$$

where the orthogonal axes are now along the local slip-line directions. Replacing $\frac{\partial}{\partial x}$ and $\frac{\partial}{\partial y}$ by the tangential dertivatives $\frac{\partial}{\partial s_\alpha}$ and $\frac{\partial}{\partial s_\beta}$ respectively along the α and β character-istics, the above equations will become independent of the orientation of axes [Ostoja-Starzewski, 1992a]. Therefore:

$$dp + 2k_\delta d\varphi = \frac{\partial k_\delta}{\partial s_\beta} ds_\alpha \qquad (2.11)$$

$$dp - 2k_\delta d\varphi = \frac{\partial k_\delta}{\partial s_\alpha} ds_\beta \qquad (2.12)$$

This stochastic system is of a quasi-linear hyperbolic type for all possible values of p and φ; it can be thus solved by means of the method of characteristics. Solution of par-ticular cases may be obtained by solving the appropriate Boundary Value Problems (BVP), when either the values or a relationship between p and φ functions are given along certain lines. These conditions are generally sufficient, but not always [Szczepinski, 1979], to define the values of p and φ uniquely in the regions adjacent to those lines, the so-called *domain of influence*. In (2.11) and (2.12), the right-hand sides are random terms.

The corresponding characteristic directions are:

$$\frac{dy}{dx} = \tan\left(\varphi + \frac{\pi}{4}\right) \qquad (2.13)$$

and

$$\frac{dy}{dx} = \tan\left(\varphi - \frac{\pi}{4}\right)$$ (2.14)

Equations (2.13) and (2.14) form the basis for the determination of the Henky-Prandtl net of slip-lines in a given Boundary Value Problem.

2.2 Solution of the Slip Line Net via Finite Difference Method

In the following, a forward finite difference approach was used, as presented in [Ostoja-Starzewski, 1992a, 1992b]. Consider a boundary (e.g. a convex one):
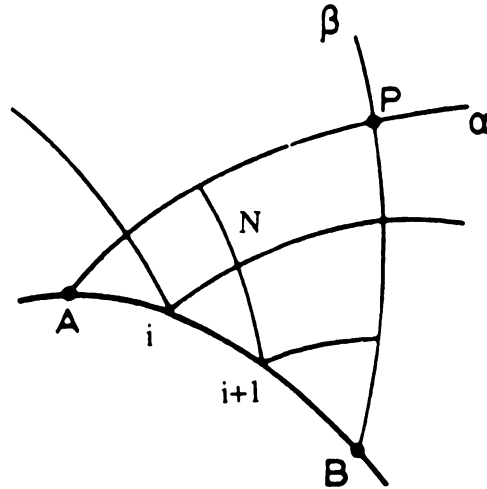

Fig. 2.2 Forward evolution
from [Kachanov, 1971]

Dividing the boundary into small and (not necessarily) equal segments, as seen in Fig. 2.2, and knowing the stress distribution along the boundary, the values of p and φ are uniquely determined at each point x_i on $\overparen{AB}$, $\left(x_i \in \overparen{AB} \right)$

Starting with two arbitrary and adjacent points, say x_i and x_{i+1} from $\overset{\frown}{AB}$, we can

set up from (2.13) and (2.14) the difference equations for coordinates x_N and y_N for the

new point of intersection N (Fig 2.3):

$$y_N - y_i = (x_N - x_i) \tan\left(\varphi_i + \frac{\pi}{4}\right) \qquad (2.15)$$

$$y_N - y_{i+1} = (x_N - x_{i+1}) \tan\left(\varphi_{i+1} - \frac{\pi}{4}\right) \qquad (2.16)$$

as well as from (2.11) and (2.12), the difference equation for p_N and φ_N:

$$p_N - p_i + 2\frac{(k_N + k_i)}{2}(\varphi_N - \varphi_i) = (k_N - k_i)\frac{ds_\alpha}{ds_\beta} \qquad (2.17)$$

$$p_N - p_{i+1} + 2\frac{(k_N + k_{i+1})}{2}(\varphi_N - \varphi_{i+1}) = (k_N - k_{i+1})\frac{ds_\beta}{ds_\alpha} \qquad (2.18)$$

Solving for p_N and φ_N, at the new point N, we get:

$$\varphi_N(\omega) = \frac{p_i - p_{i+1} + \varphi_i\left(k_N + k_i\right) + \varphi_{i+1}\left(k_N + k_{i+1}\right) + \left(k_N - k_i\right)\frac{ds_\alpha}{ds_\beta} - \left(k_N - k_{i+1}\right)\frac{ds_\alpha}{ds_\beta}}{2k_N + k_i + k_{i+1}} \qquad (2.19)$$

$$p_N(\omega) = p_i - (k_N + k_i)(\varphi_N - \varphi_i) + (k_N - k_i)\frac{ds_\alpha}{ds_\beta} \qquad (2.20)$$

where the dependence of all k's on ω is implicit and:

$$ds_\alpha = \left[(x_N - x_i)^2 + (y_N - y_i)^2 \right]^{1/2} \tag{2.21}$$

$$ds_\beta = \left[(x_N - x_{i+1})^2 + (y_N - y_{i+1})^2 \right]^{1/2} \tag{2.22}$$

and the derivatives of k with respect to s_α and s_β are treated in the finite difference sense. Note here that system (2.19) (2.20) may also be solved via backward differencing. In the following, two other schemes are also considered - one recommended by [Hill, 1950]:

$$
\begin{aligned}
y_N - y_i &= (x_N - x_i) \tan \left[(\varphi_i + \varphi_N)/2 + \pi/4 \right] \\
y_N - y_{i+1} &= (x_N - x_{i+1}) \tan \left[(\varphi_{i+1} + \varphi_N)/2 - \pi/4 \right]
\end{aligned}
\tag{2.23}
$$

and another, recommended by [Szczepinski, 1979]:

$$
\begin{aligned}
y_N - y_i &= \frac{1}{2}(x_N - x_i) \left[\tan (\varphi_i + \pi/4) + \tan (\varphi_N + \pi/4) \right] \\
y_N - y_{i+1} &= \frac{1}{2}(x_N - x_{i+1}) \left[\tan (\varphi_{i+1} - \pi/4) + \tan (\varphi_N - \pi/4) \right]
\end{aligned}
\tag{2.24}
$$

System (2.19) and (2.20) is used to determine p and φ at every point of the finite difference net. There is a random scatter in location of point N, since, according to (2.8) and (2.11), φ_1 and φ_2 are random variables:

$$\varphi_i\left(\underline{x},\,\omega\right) \;=\; \frac{1}{2}\,\mathrm{asin}\!\left(\frac{\tau_i}{k_{\delta_i}\left(\underline{x},\,\omega\right)}\right), \qquad \varphi_{i+1}\left(\underline{x},\,\omega\right) \;=\; \frac{1}{2}\,\mathrm{asin}\!\left(\frac{\tau_{i+1}}{k_{\delta_{i+1}}\left(\underline{x},\,\omega\right)}\right) \qquad (2.25)$$

This scatter is indicated by an intersection of two cones of forward evolution shown in Fig 2.3. These cones replace the characteristics of the deterministic medium problem, $\mathbf{B}_{det}$. From (2.15) (2.16) [or (2.23) or (2.24)] we can find the mean (ensemble average) coordinates of point N, by averaging in the dashed quadrangle, Fig. 2.3:
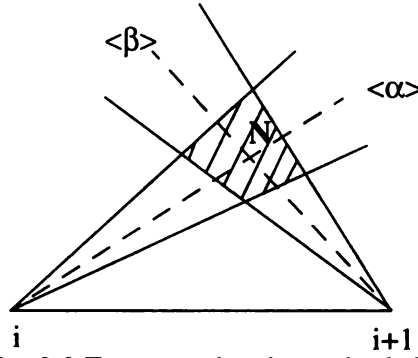
Fig. 2.3 Exact stochastic method showing
two cones of forward evolution

according to:

$$\langle x_N \rangle \;=\; \Bigg\langle \frac{y_{i+1} - y_i + x_i \tan\!\left(\varphi_i + \frac{\pi}{4}\right) - x_{i+1}\tan\!\left(\varphi_{i+1} - \frac{\pi}{4}\right)}{\tan\!\left(\varphi_i + \frac{\pi}{4}\right) - \tan\!\left(\varphi_{i+1} - \frac{\pi}{4}\right)} \Bigg\rangle \qquad (2.26)$$

$$\langle y_N \rangle \;=\; \Bigg\langle \frac{x_{i+1} - x_i + y_i\,\mathrm{ctg}\!\left(\varphi_i + \frac{\pi}{4}\right) - y_{i+1}\,\mathrm{ctg}\!\left(\varphi_{i+1} - \frac{\pi}{4}\right)}{\mathrm{ctg}\!\left(\varphi_i + \frac{\pi}{4}\right) - \mathrm{ctg}\!\left(\varphi_{i+1} - \frac{\pi}{4}\right)} \Bigg\rangle \qquad (2.27)$$

Formulas (2.26) and (2.27), derived from (2.15) and (2.16), establish the so called average characteristics or average slip-lines. The yield limit, $k_\delta(\omega)$, is taken to be a random variable which, in addition, gives randomness in p_N and φ_N as well as in x_N and y_N at the new point N which amplifies the uncertainty in the further evolution.

2.3 Limit Analysis of a Cylindrical Tube Made of a Perfectly-Plastic Material Under Internal Pressure.

2.3.1 Tube Made of a Homogeneous Material

In the following we will study a practical problem for which an analytical solution of the deterministic medium is known. Let us consider the slip-line field around a circular hole of radius a, loaded on the interior surface. Let r and θ be the polar coordinates used to describe this state of plane stress (does not depend on the z coordinate). The most general case under the above assumptions is when both σ_r and $\tau_{r\theta}$ are non-zero on the boundary. When the hole is uniformly loaded with a pressure p and a constant tangential load $\tau_{r\theta}$, the problem becomes axisymmetric.

I) The case when $\tau_{r\theta}=0$.

Since there is no tangential stress on the edge of the hole, the equilibrium condition gives $\tau_{r\theta}=0$. Therefore, at every point of the field, the principal planes have radial and circumferential directions. The slip-line will be a curve which intersects at each of its

points a ray, emerging from the centre, at an angle $\pm\frac{\pi}{4}$ [Kachanov, 1971]. But only the

logarithmic spirals exhibit this type of property:

$$\varphi - \ln\left(\frac{r}{a}\right) = \beta \tag{2.28}$$

$$\varphi + \ln\left(\frac{r}{a}\right) = \alpha \tag{2.29}$$

which generate two orthogonal families. These lines have been observed in experiments
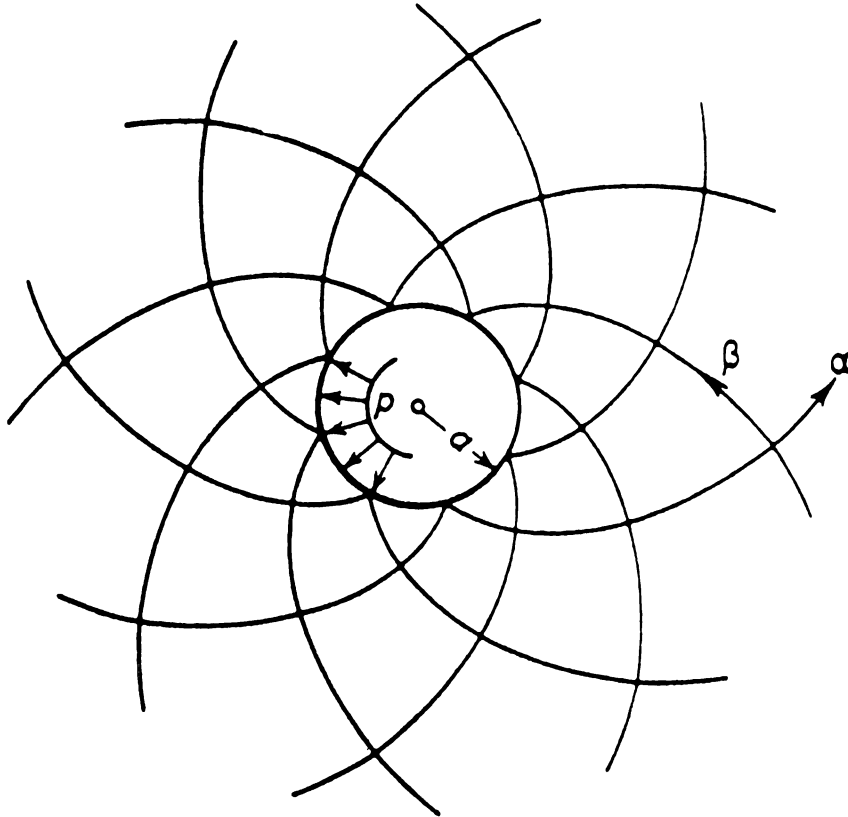
[Kachanov, 1971]:

Fig 2.4 Logarithmic Spirals [Kachanov, 1971]

For the so-called *pressure boundary conditions* in polar coordinates given by:

$$\sigma_r = -p < 0 \qquad \tau_{r\varphi} = 0 \qquad \text{at} \qquad r = a \qquad (2.30)$$

with $\sigma_\varphi > 0$, $\sigma_r < 0$ in the neighborhood of the boundary and the yield condition of the form:

$$\sigma_\varphi - \sigma_r = 2k \qquad (2.31)$$

the stresses are determined by the formulas:

$$\sigma_r = -p + 2k\ln\left(\frac{r}{a}\right) \qquad (2.32)$$

$$\sigma_\varphi = \sigma_r + 2k \qquad (2.33)$$

Note here that, if the yield condition has the form:

$$\sigma_\varphi - \sigma_r = -2k \qquad (2.34)$$

the stresses are determined by the formulas:

$$\sigma_r = (-p) - 2k\ln\left(\frac{r}{a}\right) \qquad (2.35)$$

$$\sigma_\varphi = \sigma_r - 2k \qquad (2.36)$$

From (2.32) we get:

$$\ln\left(\frac{r}{a}\right) = \frac{\sigma_r + p}{2k}$$ (2.37)

or:

$$r = ae^{\frac{\sigma_r + p}{2k}}$$ (2.38)

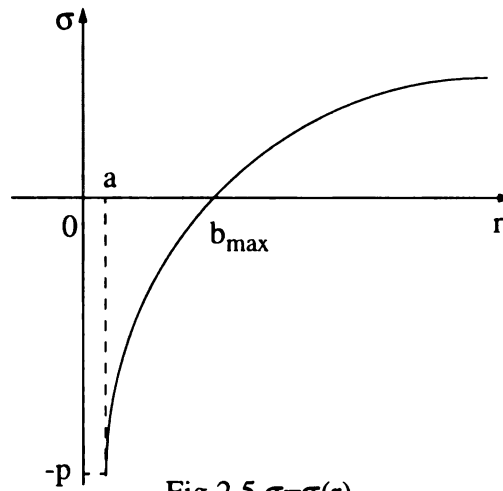The variation of $\sigma_r = \sigma_r(r)$ is shown in Fig. 2.5:

Fig 2.5 $\sigma = \sigma(r)$

From (2.38) above we can determine immediately the value of the radius $b(p^*) = b_{max}$ at which $\sigma_r = 0$:

$$b = ae^{\frac{p^*}{2k}}$$ (2.39)

II) **The case when** $\sigma_r \neq 0$, $\tau_{r\theta} \neq 0$:

The yield condition now has the form:

$$(\sigma_r - \sigma_\theta)^2 + 4\tau_{r\theta}^2 = 4k^2$$ (2.40)

and the differential equations of equilibrium can be written:

$$\frac{d\sigma_r}{dr} + \frac{\sigma_r - \sigma_\theta}{r} = 0$$ (2.41)

$$\frac{d\tau_{r\theta}}{dr} + \frac{2\tau_{r\theta}}{r} = 0$$ (2.42)

Suppose that the boundary conditions are

$$\sigma_r = -p \qquad \tau_{r\theta} = q \qquad \text{at } r = a$$ (2.43)

where, of course, $|q| \leq k$. Integrating by separation of variables in (2.42) with the BC given by (2.43), we get:

$$\tau_{r\theta} = q\left(\frac{a}{r}\right)^2 \tag{2.44}$$

From (2.40) and (2.44) we get an expression that gives the yield condition:

$$\sigma_\theta - \sigma_r = \pm\sqrt{k^2 - q^2\left(\frac{a}{r}\right)^4} \tag{2.45}$$

Substituting (2.45) in (2.41), integrating and imposing the BC, we obtain:

$$\sigma_r = -p \pm k\left[2\ln\frac{\sqrt{\left(\frac{r}{a}\right)^2 - \left(\frac{q}{k}\right)} + \sqrt{\left(\frac{r}{a}\right)^2 + \left(\frac{q}{k}\right)}}{\sqrt{1 - \left(\frac{q}{k}\right)} + \sqrt{1 + \left(\frac{q}{k}\right)}} - \left(\frac{a}{r}\right)^2\sqrt{\left(\frac{r}{a}\right)^4 - \left(\frac{q}{k}\right)^2} + \sqrt{1 - \left(\frac{q}{k}\right)^2}\right] \tag{2.46}$$

Note that when $\tau_{r\theta} = q \neq 0$, the slip-lines are no longer logarithmic spirals.

2.3.2 Tube Made of a Randomly Inhomogeneous Material

We briefly saw in the former paragraphs the analytical solution for this particular problem of a homogeneous medium (i.e. the yield limit k is constant). In case of a tube made of an inhomogeneous material, the slip-line net will have a random scatter in position given by the randomness exhibited by $k_\delta(\omega)$.

Random fluctuations in the slip-line net have been observed experimentally. An

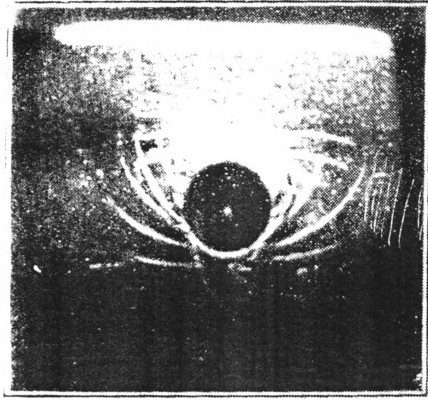example is shown in [Kachanov, 1971]:

Fig. 2.6. Random fluctuations experimentally observed
in the slip line net distribution; from [Kachanov, 1971]

The formulas (2.32) and (2.46) no longer apply and the system (2.19) and (2.20) together

with either (2.15) and (2.16) or (2.23) or (2.24) has to be used in order to determine the

slip line net and the stress field in any particular realization of a spatially inhomogenous

medium $\mathbf{B}_\delta(\omega)$ of the family $\mathbf{B}_\delta$. Recall here Fig. 2.5. The extrapolation of this result for

the case of an inhomogenous material gives a dependence of $\sigma_r = \sigma_r(r)$ according to:
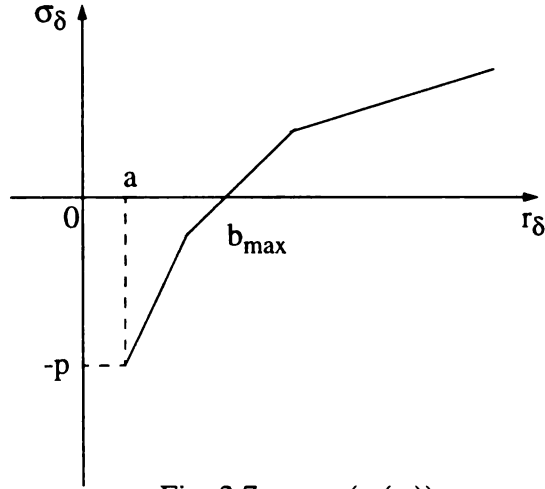
Fig. 2.7 $\sigma_\delta = \sigma_\delta(r_\delta(\omega))$

Thus the condition $\sigma_r = 0$ plays the key role in the definition of an *excursion set* of a

random field $\sigma_r(r, \varphi) = \{\sigma_r(\omega), \omega \in \Omega\}$ [Adler, 1981]:

$$A_0(\sigma_r, D) = \{ (r, \varphi) \in D | \sigma_r(r, \varphi) \geq 0 \} \tag{2.47}$$

This leads to the definition of a so-called *set of level crossing*:

$$\partial A_0(\sigma_r, D) = \{ (r, \varphi) \in D | \sigma_r(r, \varphi) = 0 \} \tag{2.48}$$

The set $\partial A_0(\sigma_r, D)$ is a set of closed contours of plastic zone, which, in the case

of a homogeneous medium with no shear loading, is a circle of radius given by (2.39):

$$b = ae^{\frac{p^*}{2k}} \tag{2.49}$$

2.3.3 The Computer Program

A computer program was developed to implement the finite difference method presented in cap 2.2.

First, the program transforms the stresses from the polar to cartesian coordinates, using the well known tensorial transformation formula:

$$\sigma = A^T \sigma' A \tag{2.50}$$

where σ and σ' designate the stress components in the cartesian and polar coordinates respectively, and A is the transformation matrix:

$$A = \begin{bmatrix} \cos\alpha & \sin\alpha \\ -\sin\alpha & \cos\alpha \end{bmatrix} \tag{2.51}$$

α being the angle between Ox and Ox'.

Next, having the stresses, the two variables p and φ can be computed at each point P_i on the boundary, using the formulas (2.6), (2.7) and (2.8), from which we get:

$$p = \frac{\sigma_x + \sigma_y}{2} \quad \text{and} \quad \phi = \frac{1}{2}\text{acos}\left(\frac{\sigma_x - \sigma_y}{2k_\delta}\right) \tag{2.52}$$

Now, having the values of p and ϕ on the boundary, using (2.19), (2.20), and either(2.15) and (2.16) or (2.23) or (2.24) of the finite difference method, we can march forward to the next row, and so on. In the end we will have all the variables p, ϕ, x and y, that uniquely determine the position and the stress components, at each point of the slip-line net. A testing follows, if $\sigma_r \geq 0$, the program draws the net and stops.

The program was tested for the homogeneous medium, by comparing the values obtained by running the program with those given by the analytical solution presented in ch. 2.3.1. A table of values for the radius b_{max} at which σ_r becomes zero is presented below. Note that the data were obtained for $\tau_{r\theta}=0$, constant k (i.e. the homogeneous medium), 60 points on the boundary, radius of hole a=1 and p=-1.9223.

Table 1: The comparison of results between the Analytical and the Finite Difference Method

#	<k(ω)>	Analytical method	Finite Difference Method	#	<k(ω)>	Analytical method	Finite Difference Method
1	1.0	2.6147	2.6158	7	1.6	1.8236	1.8239
2	1.1	2.3959	2.3961	8	1.7	1.7601	1.7605
3	1.2	2.2277	2.2272	9	1.8	1.7057	1.7060
4	1.3	2.0946	2.0950	10	1.9	1.6584	1.6588
5	1.4	1.9868	1.9874	11	2.0	1.6170	1.6174
6	1.5	1.8979	1.8985				

The mesh dependence in the case of a homogeneous medium with

$\langle k_\delta(\omega) \rangle = 1.5$, $p^* = -1.9223$, without tangential load and with internal radius of the hole
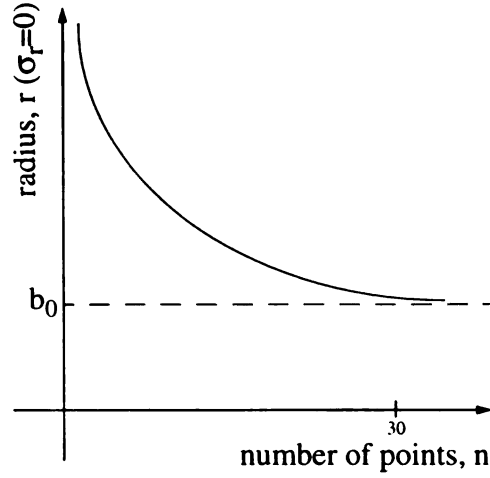
a=1, is given below:

Fig. 2.8 The dependency of the maximum radius
upon the number of points on the boundary

where b_0 is the radius obtained by the analytical solution at which $\sigma_r = 0$. The mesh

dependence has an exponential shape and for 30 points the accuracy of the finite differ-

ence method is below 3%.

2.4 Discussion of Results

In any given inhomogeneous material the set of level crossings is a random set in plane, which, due to the spatial homogeneity of field k_δ, is a circle containing all the possibilities. Let b_{max} and b_{min} be the maximum and minimum distance for a given realization, respectively, from the origin to the contour. Since b_{max} determines the minimal amount of material needed for a tube to withstand the internal pressure p^*, the natural questions to ask are:

Q1: "Is $b_{max}(p^*)$ smaller, equal to, or larger than $b(p^*)$ of the homogeneous medium problem?"

Q2: "What is the probability distribution of b_{max} and b_{min}?"

Q3: "What is the effect of shear traction in boundary condition (2.43) versus (2.30)?"

Two particular cases of noise were investigated

$$k_\delta' \in [-0.0094, 0.0094] \qquad (2.53)$$

and

$$k_\delta' \in [-0.025, 0.025] \qquad (2.54)$$

Figures 2.9. a) and b) show the slip-line net of the tube made of a homogeneous material that withstands a normal pressure $p^* = -3$ and a normal and tangential loading $p^* = -3$ and $q^* = 1.3$, respectively. The slip-line networking correspond to

$\langle k_\delta(\omega) \rangle$ = 1.5 and internal radius a=1. As one expects, the amount of material needed (i.e. the radius of the slip-line net) is greater when we have besides normal loading a tangential one. For an infinite number of points on the internal boundary, the outer boundary at which σ_r = 0 will be a circle of radius given by either (2.39) (i.e. no shear loading) or a similar expression derived for the case when $\sigma_r \neq 0$, $\tau_{r\theta} \neq 0$ on the outer boundary.

Figures 2.10 a) b) show the slip-line net given by a single realization $\mathbf{B}_\delta(\omega)$ of a random medium with $\langle k_\delta \rangle$ = 1.5 and k_δ' sampled according to (2.54).
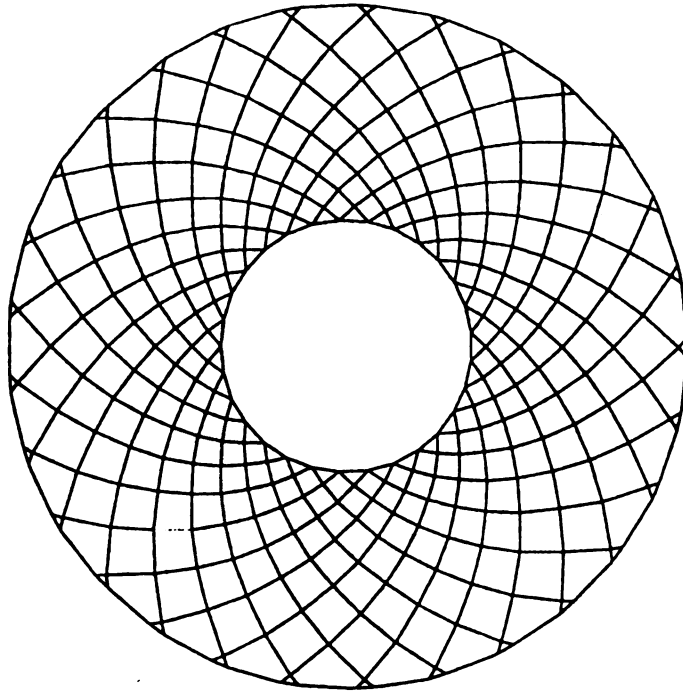
a)
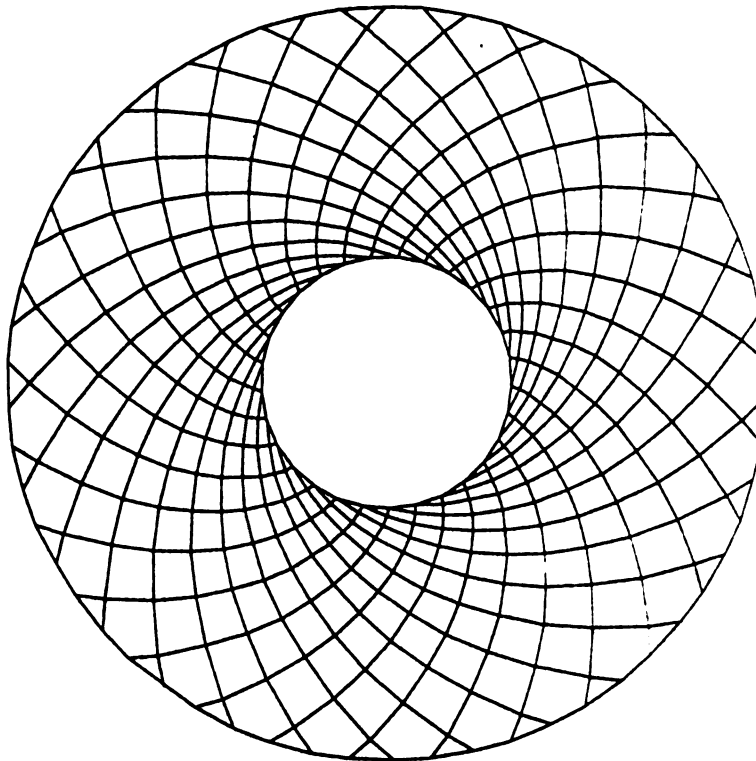
b)

Fig. 2.9. Slip line patterns in a homogenous material under: a) pressure boundary conditions (2.30) and b) hydrostatic pressure and shear boundary conditions (2.43)
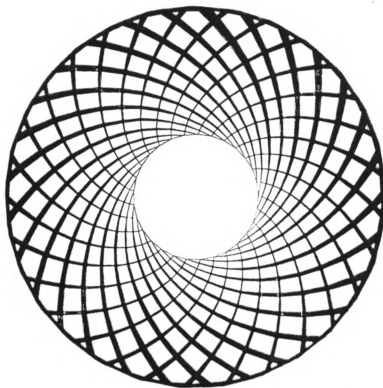
a)

b)
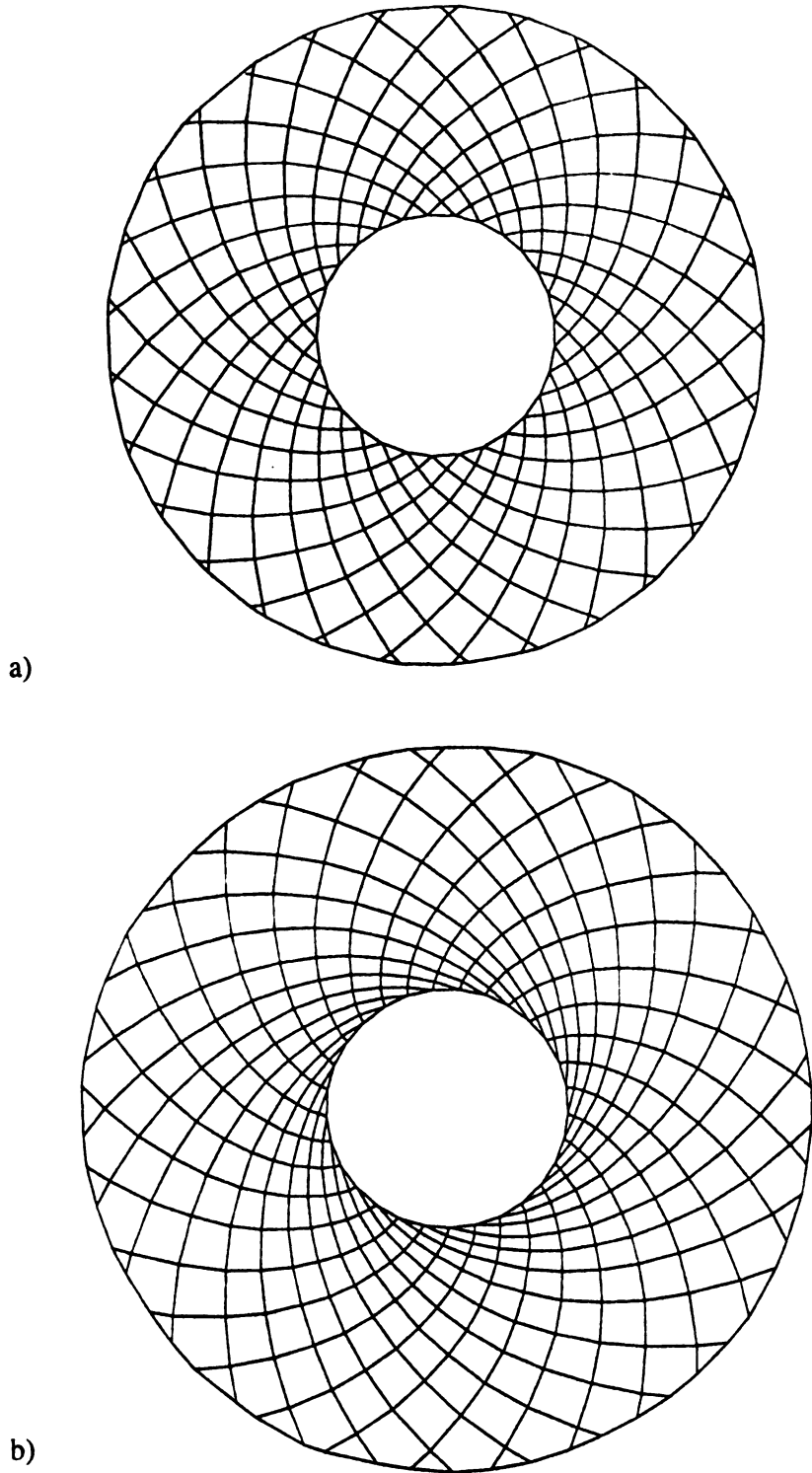
Fig. 2.10. Slip line patterns in a randomly inhomogenous material under: a) pressure boundary conditions (2.30) and b) hydrostatic pressure and shear boundary conditions (2.43). In each case, a single realization of $B_\delta(\omega)$ is used.

In Fig. 2.11 a) we plot patterns of slip-lines under boundary condition (2.30) corresponding to four hundred realizations $B_\delta(\omega)$ of a random medium with $\langle k_\delta(\omega) \rangle = 1.5$ and k_δ' sampled according to (2.54). The set of level crossings is shown as a ring containing all four hundred piecewise-constant non-circular closed curves. Next, in Fig. 2.11 b) we plot slip-line patterns for the same type of medium under boundary condition (2.43) also for four hundred realizations.
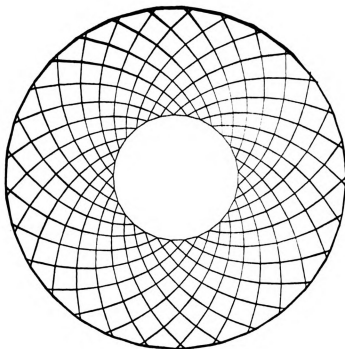
a)

b)

Fig 2.11. Slip line patterns in a randomly inhomogenous material under: a) pressure boundary conditions (2.30) and b) hydrostatic pressure and shear boundary conditions (2.43). In each case, four hundred realization of $B_8(\omega)$ are used.

It is immediately seen that the tangential loading produces a sensitive increase in the scatter of the slip-line net.

Finally, in Figs. 2.12 a) and b) we plot probability distributions of b_{max} and b_{min} for the cases, respectively, of the pressure boundary condition (2.30), and b) of the pressure and traction boundary condition (2.43). In order to demonstrate the sensitivity to random noise in the yield function, in each one of these two figures we show data corresponding to (2.53) and (2.54).

a) $b(p^*) = 2.723$

b) $b(p^*, q^*) = 3.028$
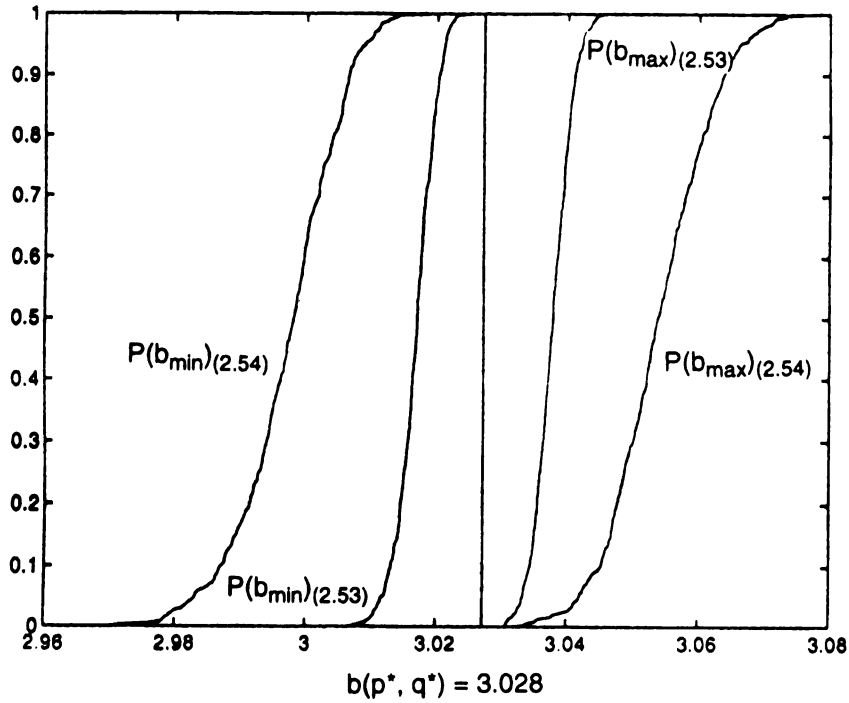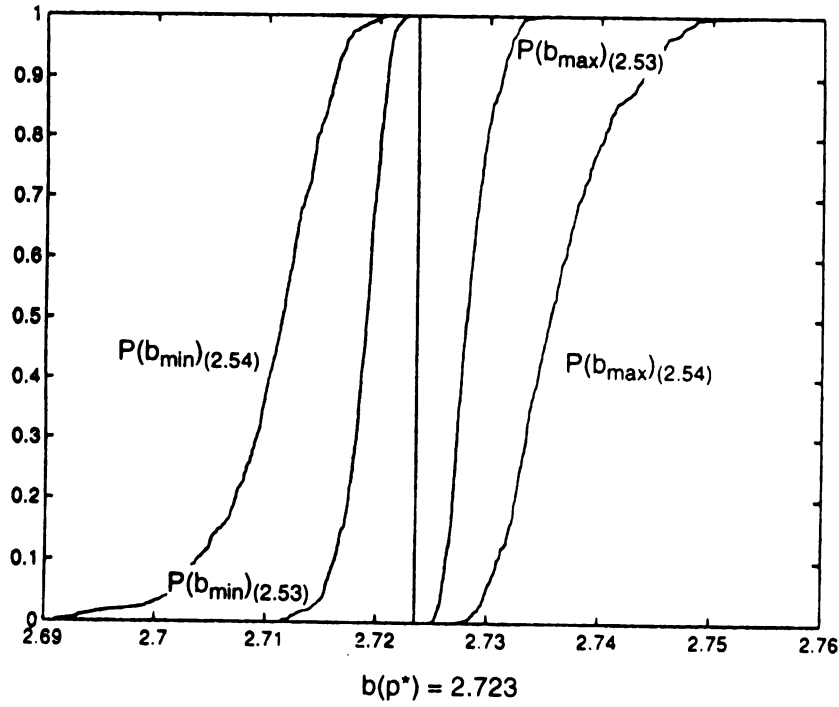
Fig 2.12 Probability distributions $P(b_{max})_{(2.53)}$, $P(b_{max})_{(2.54)}$, $P(b_{min})_{(2.53)}$, and $P(b_{min})_{(2.54)}$ for the case a) of pressure boundary condition (2.30). and b) pressure and shear boundary condition (2.43); k_δ is sampled according to (2.53) and (2.54). In each case four hundred realizations of $B(\omega)$ are used. Also. the deterministic cases $b(p^*) = 2.723$ and $b(p^*, q^*) = 3.028$ are shown.

It follows now that the answer to the first question is "always larger", whereby b_{max} increases as the noise level in $k_\delta{}'$ increases. Thus, the principal conclusion is that the presence of material inhomogeneities requires a thicker tube than what is predicted by the homogeneous medium theory. Let us note here that the higher the pressure p, the greater is the external radius b, and hence, the greater is the spread of the forward evolution cones implying an increase in the scatter of b_{max} and b_{min}. Interestingly, both random variables b_{max} and b_{min} are symmetrically distributed about the deterministic radius b(p*) of the homogeneous medium problem; this answers Q2. The same qualitative conclusions carry over to the case of the pressure and shear boundary condition, but one must note here that the addition of shear traction has a strongly amplifying effect on the scatter of dependent field quantities, and, most notably, on the spread of slip-lines - compare Fig. 2.11 a) and b); this addresses Q3.

We observed that the choice of the forward (as used here) versus backward differencing scheme has only a small effect on the solution. The results outlined above are in accord with those obtained by [Ostoja-Starzewski, 1992a, 1992b], namely that in the case of inhomogeneous boundary data, the sensitivity of field quantities to the 'magnitude' of the randomness of plastic limit k increases as this randomness grows.

3. PLASTICITY OF GRANULAR MEDIA

3.1 Basic Concepts

Statics of granular media studies two types of stress states: stress states in which a small change in body or surface forces do not destroy the state of equilibrium and stress states in which a change, no matter how small, in the applied forces causes a loss of equilibrium. The ones that lie in the second category, the so-called limiting stress states, depend directly on the basic mechanical constraints which characterize the resistance of a granular material to shear deformation and form the basis of the theory of limiting equilibrium

In 1773, Coulomb, the originator of this theory, formulated the basic theorems of limiting equilibrium. Later in 1857, Rankine introduced the concept of slip surfaces and found the condition of limiting equilibrium.

Let us now take a look at a point P in a granular medium and consider an element of area containing this point. This area element is loaded with a stress vector p which forms with the normal n to the surface an angle δ as can be seen in Fig. 3.1:
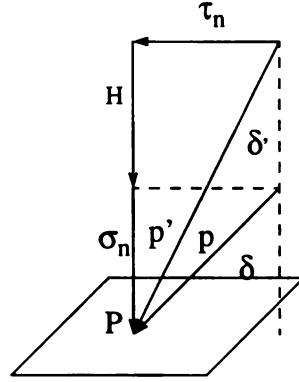
Fig.3.1 Limiting Condition

The components of the stress vector p are σ_n and τ_n. The experiments show that the resistance to shear over this area in a granular medium with some cohesion can be expressed as

$$|\tau_n| = \sigma_n \tan\rho + H_0 \tag{3.1}$$

which applies when the equilibrium is about to be destroyed. This resistance consists of a resistance from internal friction and a resistance from cohesion H_0.

The constants ρ and H_0 are the angle of internal friction and the coefficient of cohesion, respectively, and they can be looked upon simply as parameters which characterize the total resistance of the granular medium to shear. There are two special cases: if $H_0=0$ the medium is cohesionless and when $\rho=0$ the medium is an ideally cohesive, one described by (2.4).

It was shown [Sokolowskii, 1965] that no slip occurs if:

$$\left|\tau_n\right| \le \sigma_n \tan\rho + H_0 \qquad (3.2)$$

where

$$\sigma_n \ge -H_0 \cot\rho \qquad (3.3)$$

Define now:

$$H = H_0 \cot\rho \qquad (3.4)$$

where H is the ultimate resistance to uniform three-dimensional tension [Sokolowskii, 1965].

Assuming that there is an equivalent stress vector p' acting on the element of area at an angle δ' with the normal n, its components are $\sigma_n + H$ and τ_n. Inequality (3.2) becomes:

$$\left|\tau_n\right| \le (\sigma_n + H)\tan\rho \qquad (3.5)$$

where $\sigma_n \ge -H$

The special limiting equilibrium is given when equation (3.5) has the form:

$$|\tau_n| = (\sigma_n + H) \tan\rho \qquad (3.6)$$

Equation (3.6) can be expressed [Sokolowskii,1965] as:

$$\frac{1}{4}(\sigma_x - \sigma_y)^2 + \tau_{xy}^2 = \frac{(\sin\rho)^2}{4}(\sigma_x + \sigma_y + 2H)^2 \qquad (3.7)$$

which is the well known Mohr-Coulomb yield criterion.

3.2 Continuum Field Equations

The field equations of equilibrium are:

$$\frac{\partial\sigma_x}{\partial x} + \frac{\partial\tau_{xy}}{\partial y} = \gamma\sin\alpha \qquad (3.8)$$

$$\frac{\partial\sigma_y}{\partial y} + \frac{\partial\tau_{xy}}{\partial x} = \gamma\cos\alpha \qquad (3.9)$$

where γ is the density of the medium and α is, for generality, the angle between x axis and the horizontal.

At this point, two variables σ and φ are introduced [Sokolovskii, 1965]:

$$\sigma_x = \sigma(1 + \sin\rho\cos2\varphi) - H \tag{3.10}$$

$$\sigma_y = \sigma(1 - \sin\rho\cos2\varphi) - H \tag{3.11}$$

$$\tau_{xy} = \sigma\sin\rho\sin2\varphi \tag{3.12}$$

We observe that if the value of σ is sufficiently large, the coefficient H will cease to have any real influence on the stress components and in this case, it can be neglected. Therefore, as σ increases, the limiting equilibrium tends to the corresponding limiting equilibrium of an ideal granular medium.

In the development of this chapter we will consider ρ and H as random fields, namely:

$$\rho_\delta(\underline{x}, \omega) = \langle\rho_\delta(\underline{x}, \omega)\rangle + \rho'_\delta(\underline{x}, \omega), \quad \langle\rho'_\delta(\underline{x}, \omega)\rangle = 0 \tag{3.13}$$

$$H_\delta(\underline{x}, \omega) = \langle H_\delta(\underline{x}, \omega)\rangle + H'_\delta(\underline{x}, \omega), \quad \langle H'_\delta(\underline{x}, \omega)\rangle = 0 \tag{3.14}$$

Formulas (3.10), (3.11) and (3.12) satisfy identically the Mohr-Coulomb yield criterion (3.7).

3.3 Cauchy Problem of a Homogeneous Granular Medium

In the case of a homogeneous material, H and ρ are constants, and their values depend on the particular material. In the following, an analytical method to solve for the slip-line net was developed.

For a weightless homogeneous medium, the differential equations for the two characteristics are [Sokolovskii,1965]:

$$d\sigma \mp 2\sigma \tan\rho \cdot d\varphi = 0 \tag{3.15}$$

which can be integrated by separating the variables:

$$\sigma \cdot e^{\mp 2\tan(\rho)\varphi} = \text{constant} \tag{3.16}$$

where equation (3.16) holds along an α (β) line (see Fig. 3.2).

Now, if the stresses (i.e. σ_x, σ_y, τ_{xy}) are given along a boundary, say AB (recall here Fig. 2.2) which is divided into n segments, then the two variables σ and ρ can be computed at every single point along that boundary. Marching forward, from every two adjacent points, say i and i+1, on the boundary, the next point N can be found:
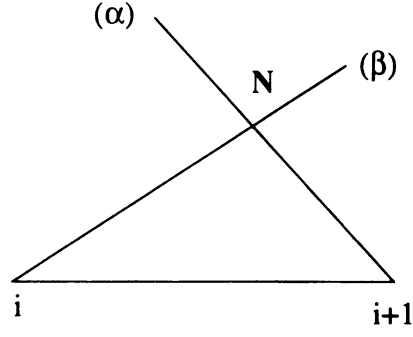
Fig 3.2 Forward evolution for a
deterministic medium.

From (3.16) we get:

$$\sigma_N = \mp\sqrt{\sigma_i\sigma_{i+1}e^{2(\tan\rho_i\varphi_i - \tan\rho_{i+1}\varphi_{i+1})}} \tag{3.17}$$

$$\varphi_N = \frac{1}{2\tan\rho_N}\left[\ln\left(\frac{\sigma_i}{\sigma_N}\right) + 2\tan(\rho_i)\,\varphi_i\right] \tag{3.18}$$

or:

$$\varphi_N = \frac{1}{2\tan\rho_N}\left[\ln\left(\frac{\sigma_N}{\sigma_{i+1}}\right) + 2\tan(\rho_{i+1})\,\varphi_{i+1}\right] \tag{3.19}$$

Introducing the auxiliary angle ε:

$$2\varepsilon = \frac{\pi}{2} - \rho \tag{3.20}$$

the angle between the two slip-lines, α and β, and the x axis will be respectively:

$$\varphi \mp \varepsilon \qquad\qquad (3.21)$$

Equations (3.17), (3.18) or (3.19) together with:

$$dy = dx \tan (\varphi \mp \varepsilon) \qquad\qquad (3.22)$$

allow us to find the slip-line net within the *domain of influence*.

The family of characteristics given by the upper signs are called the first family or α characteristics, while the family given by the lower signs, the second or the β characteristics. The basic set of equations has two real different families of characteristics and are, consequently, quasi-linear hyperbolic differential equations.

In the region under consideration, the xOy plane, the two sets of slip-lines intersect at each and every point through which they pass at an angle 2ε and hence the whole region is covered by a network of slip-lines.

3.4 Inhomogeneous Continuum Model

Consider a random medium $\mathbf{B} = \{\mathbf{B}(\omega), \omega \in \Omega\}$, where ω is an element of the probability space Ω. The random yield function:

$$F_\delta(\sigma(\omega)) = 0 \tag{3.23}$$

which is generally known to have a Mohr-Coulomb form for granular media, is approximated by:

$$\frac{1}{4}(\sigma_x - \sigma_y)^2 + \tau_{xy}^2 = \frac{(\sin\rho_\delta)^2}{4}(\sigma_x + \sigma_y + 2H_\delta)^2 \tag{3.24}$$

where ρ_δ and H_δ are two random fields:

$$\rho_\delta(\underline{x}, \omega) = \langle \rho_\delta(\underline{x}, \omega) \rangle + \rho'_\delta(\underline{x}, \omega), \quad \langle \rho'_\delta(\underline{x}, \omega) \rangle = 0 \tag{3.25}$$

$$H_\delta(\underline{x}, \omega) = \langle H_\delta(\underline{x}, \omega) \rangle + H'_\delta(\underline{x}, \omega), \quad \langle H'_\delta(\underline{x}, \omega) \rangle = 0 \tag{3.26}$$

By assuming a scatter in the values of $\rho_\delta(\underline{x}, \omega)$ and $H_\delta(\underline{x}, \omega)$, we will study the effects of the material randomness upon the slip-line nets for materials that obey the Mohr-Coulomb yield criterion.

The equilibrium equations (3.8) and (3.9) can be written for a weightless medium (i.e. $\gamma=0$) as:

$$\frac{\partial \sigma_x}{\partial x} + \frac{\partial \tau_{xy}}{\partial y} = 0 \tag{3.27}$$

$$\frac{\partial \sigma_y}{\partial y} + \frac{\partial \tau_{xy}}{\partial x} = 0 \tag{3.28}$$

Substituting equations (3.10), (3.11) and (3.12) in (3.27) and (3.28) above, we get:

$$[1 + \sin\rho\cos 2\varphi]\frac{\partial \sigma}{\partial x} + \sin\rho\sin 2\varphi\frac{\partial \sigma}{\partial y} - 2\sigma\sin\rho\left(\sin 2\varphi\frac{\partial \varphi}{\partial x} - \cos 2\varphi\frac{\partial \varphi}{\partial y}\right)$$
$$+ \sigma\cos\rho\left(\cos 2\varphi\frac{\partial \rho}{\partial x} + \sin 2\varphi\frac{\partial \rho}{\partial y}\right) - \frac{\partial H}{\partial x} = 0 \tag{3.29}$$

$$\sin\rho\sin 2\varphi\frac{\partial \sigma}{\partial x} + (1 - \sin\rho\cos 2\varphi)\frac{\partial \sigma}{\partial y} + 2\sigma\sin\rho\left(\cos 2\varphi\frac{\partial \varphi}{\partial x} + \sin 2\varphi\frac{\partial \varphi}{\partial y}\right)$$
$$+ \sigma\cos\rho\left(\sin 2\varphi\frac{\partial \rho}{\partial x} - \cos 2\varphi\frac{\partial \rho}{\partial y}\right) - \frac{\partial H}{\partial y} = 0 \tag{3.30}$$

Several attempts to adapt and generalize some existing methods of obtaining the equations of characteristics for the case of a deterministic medium to our randomly inhomogeneous granular medium were made. They are presented below.

3.4.1 Nedderman's approach

Multiplying (3.29) by $[1 - \sin\rho\cos 2\varphi]$, (3.30) by $[-\sin\rho\sin 2\varphi]$ and adding them, one gets:

$$\frac{\partial \sigma}{\partial x}(\cos\rho)^2 = 2\sigma\sin\rho\left[\sin 2\varphi\frac{\partial \varphi}{\partial x} + (\sin\rho - \cos 2\varphi)\frac{\partial \varphi}{\partial y}\right] \tag{3.31}$$
$$-\sigma\cos\rho\left[(\cos 2\varphi - \sin\rho)\frac{\partial \rho}{\partial x} + \sin 2\varphi\frac{\partial \rho}{\partial y}\right]$$
$$+ \frac{\partial H}{\partial x}(1 - \sin\rho\cos 2\varphi) - \frac{\partial H}{\partial y}\sin\rho\sin 2\varphi$$

Multiplying (3.29) by $[-\sin\rho\sin 2\varphi]$, (3.30) by $[1 + \sin\rho\cos 2\varphi]$ and adding them, one obtains:

$$\frac{\partial\sigma}{\partial y}(\cos\rho)^2 = -2\sigma\sin\rho\left[(\sin\rho + \cos 2\varphi)\frac{\partial\varphi}{\partial x} + \sin 2\varphi\frac{\partial\varphi}{\partial y}\right]$$

$$+ \sigma\cos\rho\left[-\sin 2\varphi\frac{\partial\rho}{\partial x} + (\cos 2\varphi + \sin\rho)\frac{\partial\rho}{\partial y}\right]$$

$$-\frac{\partial H}{\partial x}\sin\rho\sin 2\varphi + \frac{\partial H}{\partial y}(1 + \sin\rho\cos 2\varphi) \qquad (3.32)$$

Now, making use of the angle ξ and of the property:

$$\frac{d\sigma}{ds} = \frac{\partial\sigma}{\partial x}\cos\xi + \frac{\partial\sigma}{\partial y}\sin\xi \qquad (3.33)$$

from (3.31) and (3.32) we get:

$$\frac{d\sigma}{ds}(\cos\rho)^2 = 2\sigma\sin\rho\,[\sin(2\varphi - \xi) - \sin\rho\sin\xi]\frac{1}{\cos\xi}\frac{d\varphi}{ds} \qquad (3.34)$$

$$-\sigma\cos\rho\,[\cos(2\varphi - \xi) - \sin\rho\cos\xi]\frac{1}{\cos\xi}\frac{d\rho}{ds}$$

$$+ \left[1 - \sin\rho\cos(2\varphi - \xi)\frac{1}{\cos\xi}\right]\frac{dH}{ds}$$

$$+ 2\sigma\sin\rho\,\{-[\sin(2\varphi - \xi) - \sin\rho\sin\xi]\tan\xi + [\sin\rho\cos\xi - \cos(2\varphi - \xi)]\}\frac{\partial\varphi}{\partial y}$$

$$+ \sigma\cos\rho\,\{[\cos(2\varphi - \xi) - \sin\rho\cos\xi]\tan\xi - [\sin(2\varphi - \xi) - \sin\rho\sin\xi]\}\frac{\partial\rho}{\partial y}$$

$$+ [\sin\rho\cos(2\varphi - \xi)\tan\xi - [-\sin\rho\sin(2\varphi - \xi)]]\frac{\partial H}{\partial y}$$

It can be now seen that if the coefficients of $\frac{\partial \varphi}{\partial y}$, $\frac{\partial \rho}{\partial y}$ and $\frac{\partial H}{\partial y}$ respectively vanish, the equation (3.34) becomes an ordinary differential equation. For the homogeneous case this happens when $\xi = \varphi \pm \varepsilon$, where ε is given by equation (3.20), therefore, for that value of ξ, there are two directions (i.e. the characteristics) along which equation (3.34) reduces to an ordinary differential equation. It can, however, be easily verified that, in the case of an inhomogeneous medium, the other two coefficients vanish at a different value of angle ξ, namely when $\xi = \varphi$. Therefore, equation (3.34) cannot further be utilized.

3.4.2 Sokolowskii's approach

Multiplying equations (3.29) and (3.30) by $\sin(\varphi \pm \varepsilon)$ and $\cos(\varphi \pm \varepsilon)$ respectively, and using the trigonometric identities:

$$\sin(\varphi \pm \varepsilon) = \sin(\varphi \mp \varepsilon)\cos 2\varepsilon \pm \sin 2\varepsilon \cos(\varphi \mp \varepsilon) \tag{3.35}$$

$$\cos(\varphi \pm \varepsilon) = \cos(\varphi \mp \varepsilon)\cos 2\varepsilon \mp \sin 2\varepsilon \sin(\varphi \mp \varepsilon) \tag{3.36}$$

one gets:

$$\left[\frac{\partial \sigma}{\partial x} \mp 2\sigma\tan\rho\frac{\partial \varphi}{\partial x} \pm \sigma\frac{\partial \rho}{\partial y} - \frac{\partial H}{\partial x} \pm \frac{\partial H}{\partial y}\tan\rho\right]\cos(\varphi \mp \varepsilon) \tag{3.37}$$
$$+ \left[\frac{\partial \sigma}{\partial y} \mp 2\sigma\tan\rho\frac{\partial \varphi}{\partial y} \mp \sigma\frac{\partial \rho}{\partial x} \mp \frac{\partial H}{\partial x}\tan\rho - \frac{\partial H}{\partial y}\right]\sin(\varphi \mp \varepsilon) = 0$$

Equation (3.37) reduces, for the case of the homogeneous media, to equation (3.15). However, when φ and H are random fields (i.e. inhomogeneous media), we see that equation (3.37) contains mixed partial derivatives, and the method reaches a dead end.

3.4.3 Proposed approach: the method used for HMH materials (ch. 2), adapted to granular media.

In this section we will present a method similar to the one developed in [Ostoja-Starzewski, 1992a] and already used in the second chapter of this thesis. Substituting equations (3.10), (3.11) and (3.12) in (3.27) and (3.28) above, differentiating and setting φ = −ε, we get:

$$[1 + (\sin\rho)^2]\frac{\partial\sigma}{\partial x} - \sin\rho\cos\rho\frac{\partial\sigma}{\partial y} + 2\sigma\sin\rho\left(\cos\rho\frac{\partial\varphi}{\partial x} + \sin\rho\frac{\partial\varphi}{\partial y}\right)$$

$$+ \sigma\cos\rho\left(\sin\rho\frac{\partial\rho}{\partial x} - \cos\rho\frac{\partial\rho}{\partial y}\right) - \frac{\partial H}{\partial x} = 0 \qquad (3.38)$$

$$-\sin\rho\cos\rho\frac{\partial\sigma}{\partial x} + (\cos\rho)^2\frac{\partial\sigma}{\partial y} + 2\sigma\sin\rho\left(\sin\rho\frac{\partial\varphi}{\partial x} - \cos\rho\frac{\partial\varphi}{\partial y}\right) \qquad (3.39)$$

$$-\sigma\cos\rho\left(\cos\rho\frac{\partial\rho}{\partial x} + \sin\rho\frac{\partial\rho}{\partial y}\right) - \frac{\partial H}{\partial y} = 0$$

Here, the rectangular axes are now along the local slip-line directions. Replacing $\frac{\partial}{\partial x}$ and $\frac{\partial}{\partial y}$ by the tangential dertivatives $\frac{\partial}{\partial s_\alpha}$ and $\frac{\partial}{\partial s_\beta}$ along the α and β characteristics, the above equations will become independent of the orientation of axes. Therefore, we

get:

$$\left[1 + (\sin\rho)^2 - \sin\rho\cos\rho\frac{ds_\alpha}{ds_\beta}\right]d\sigma + 2\sigma\sin\rho\left(\cos\rho + \sin\rho\frac{ds_\alpha}{ds_\beta}\right)d\varphi$$
$$+ \sigma\cos\rho\left(\sin\rho - \cos\rho\frac{ds_\alpha}{ds_\beta}\right)d\rho - dH = 0 \qquad (3.40)$$

$$\left[-\sin\rho\cos\rho\frac{ds_\beta}{ds_\alpha} + (\cos\rho)^2\right]d\sigma + 2\sigma\sin\rho\left(\sin\rho\frac{ds_\beta}{ds_\alpha} - \cos\rho\right)d\varphi \qquad (3.41)$$
$$- \sigma\cos\rho\left(\cos\rho\frac{ds_\beta}{ds_\alpha} + \sin\rho\right)d\rho - dH = 0$$

The corresponding directions of the two families of characteristics, α and β, are:

$$dy = dx\tan(\varphi \mp \varepsilon) \qquad (3.42)$$

System (3.40), (3.41) can be solved by using a finite difference approach. Denoting the coefficients of $d\sigma$, $d\varphi$ and $d\rho$ in (3.40) and (3.41) as A_2, B_2, C_2 and A_1, B_1, C_1, respectively, equations (3.40) and (3.41) can be written:

$$A_2 d\sigma + 2\langle\sigma\rangle B_2 d\varphi + \langle\sigma\rangle C_2 d\rho - dH = 0 \qquad (3.43)$$

$$A_1 d\sigma + 2\langle\sigma\rangle B_1 d\varphi - \langle\sigma\rangle C_1 d\rho - dH = 0 \qquad (3.44)$$

where:

$$A_1 = -\sin\left(\frac{\rho_N + \rho_1}{2}\right)\cos\left(\frac{\rho_N + \rho_1}{2}\right)\frac{ds_\beta}{ds_\alpha} + \left[\cos\left(\frac{\rho_N + \rho_1}{2}\right)\right]^2 \tag{3.45}$$

$$B_1 = \sin\left(\frac{\rho_N + \rho_1}{2}\right)\left[\sin\left(\frac{\rho_N + \rho_1}{2}\right)\frac{ds_\beta}{ds_\alpha} - \cos\left(\frac{\rho_N + \rho_1}{2}\right)\right] \tag{3.46}$$

$$C_1 = \cos\left(\frac{\rho_N + \rho_1}{2}\right)\left[\cos\left(\frac{\rho_N + \rho_1}{2}\right)\frac{ds_\beta}{ds_\alpha} + \sin\left(\frac{\rho_N + \rho_1}{2}\right)\right] \tag{3.47}$$

$$A_2 = 1 + \left[\sin\left(\frac{\rho_N + \rho_2}{2}\right)\right]^2 - \sin\left(\frac{\rho_N + \rho_2}{2}\right)\cos\left(\frac{\rho_N + \rho_2}{2}\right)\frac{ds_\alpha}{ds_\beta} \tag{3.48}$$

$$B_2 = \sin\left(\frac{\rho_N + \rho_2}{2}\right)\left[\cos\left(\frac{\rho_N + \rho_2}{2}\right) + \sin\left(\frac{\rho_N + \rho_2}{2}\right)\frac{ds_\alpha}{ds_\beta}\right] \tag{3.49}$$

$$C_2 = \cos\left(\frac{\rho_N + \rho_2}{2}\right)\left[\sin\left(\frac{\rho_N + \rho_2}{2}\right) - \cos\left(\frac{\rho_N + \rho_2}{2}\right)\frac{ds_\alpha}{ds_\beta}\right] \tag{3.50}$$

System (3.43) and (3.44) can be solved by using a finite difference approach. Thus, the two parameters, σ_N and φ_N at the new point N are given by:

$$\sigma_N = \frac{H_N - H_2 + \sigma_2\left(A_2 - B_2(\varphi_N - \varphi_2) + \frac{C_2}{2}(\rho_N - \rho_2)\right)}{A_2 + B_2(\varphi_N - \varphi_2) - \frac{C_2}{2}(\rho_N - \rho_2)} \tag{3.51}$$

$$\varphi_N = \varphi_1 + \frac{H_N - H_1 - A_1(\sigma_N - \sigma_1) - \frac{(\sigma_N + \sigma_1)}{2}C_1(\rho_N - \rho_1)}{(\sigma_N + \sigma_1)B_1} \tag{3.52}$$

where the dependency of all ρ's and H's on ω is implicit.

Using (3.51) and (3.52), one can determine both σ and φ at every next point of the finite difference net. Having σ and φ all over the net, one can find the coordinates x_N and y_N of the new point N:

$$\langle x_N \rangle = \left\langle \frac{y_{i+1} - y_i + x_i \tan\left(\varphi_i + \frac{\pi}{4}\right) - x_{i+1} \tan\left(\varphi_{i+1} - \frac{\pi}{4}\right)}{\tan\left(\varphi_i + \frac{\pi}{4}\right) - \tan\left(\varphi_{i+1} - \frac{\pi}{4}\right)} \right\rangle \tag{3.53}$$

$$\langle y_N \rangle = \left\langle \frac{x_{i+1} - x_i + y_i \operatorname{ctg}\left(\varphi_i + \frac{\pi}{4}\right) - y_{i+1} \operatorname{ctg}\left(\varphi_{i+1} - \frac{\pi}{4}\right)}{\operatorname{ctg}\left(\varphi_i + \frac{\pi}{4}\right) - \operatorname{ctg}\left(\varphi_{i+1} - \frac{\pi}{4}\right)} \right\rangle \tag{3.54}$$

as well as the stress distribution by using formulas (3.10), (3.11) and (3.12). System (3.53) and (3.54) establishes the average coordinates of the slip-line net.

However, it was found that in the case of granular media, whose behavior is approximated by the Mohr-Coulomb yield criterion, the differencing scheme given by (2.15) and (2.16):

$$y_N - y_i = (x_N - x_i) \tan\left(\varphi_i + \frac{\pi}{4}\right) \tag{3.55}$$

$$y_N - y_{i+1} = (x_N - x_{i+1}) \tan\left(\varphi_{i+1} - \frac{\pi}{4}\right)$$

that give (3.53) and (3.54), does not stabilize the slip-line net with respect to the number of points that are chosen on the boundary. Moreover, the scheme proposed by (Hill, 1950),

i.e. formulas (2.23):

$$y_N - y_i = (x_N - x_i) \tan [(\varphi_i + \varphi_N) / 2 + \pi/4]$$

$$y_N - y_{i+1} = (x_N - x_{i+1}) \tan [(\varphi_{i+1} + \varphi_N) / 2 - \pi/4]$$

(3.56)

shows the same weakness. Interestingly, by using instead the scheme proposed by [Szczepinski, 1979], i.e. formulas (2.24):

$$y_N - y_i = \frac{1}{2} (x_N - x_i) [\tan (\varphi_i + \pi/4) + \tan (\varphi_N + \pi/4)]$$

$$y_N - y_{i+1} = \frac{1}{2} (x_N - x_{i+1}) [\tan (\varphi_{i+1} - \pi/4) + \tan (\varphi_N - \pi/4)]$$

(3.57)

solution of the deterministic boundary value problem converges to the analytical one as the number of points on the boundary increases.

In order to verify the computer program as well as the accuracy of the finite difference method, a problem for which an analytical solution exists was solved. The problem (Sokolovskii, 1965, ch 1, pp49) is presented below:
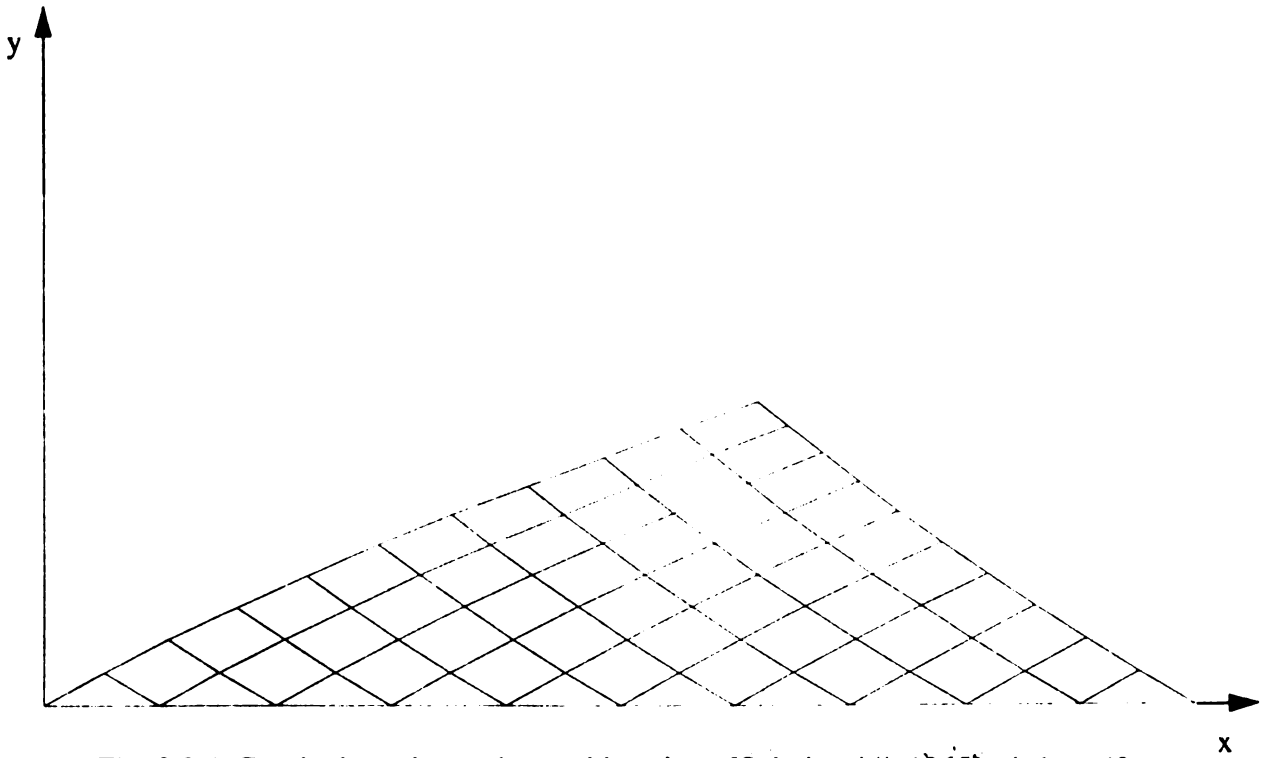
Fig. 3.3 A Cauchy boundary value problem from [Sokolovskii. 1965], ch 1, pp49

The input data for the ith point on the boundary were as follows:

$$p(i) = 2 + (i-1) \cdot \frac{2}{n-1} \qquad (3.58)$$

$$\varphi(i) = 0 \qquad (3.59)$$

$$x(i) = (i-1)\frac{1}{n-1} \qquad (3.60)$$

$$y(i) = 0 \qquad (3.61)$$

It was observed that the finite difference method gives very accurate results for this

problem, with an error of less than 3%. This suggests that the finite difference method is

suitable for the study of the effects caused by the randomness in material properties upon

the slip line net distribution. The analyzed problem in case where randomness exists is

presented below. The noise was taken to be $\rho_\delta' \in [-0.375, 0.375]$, and

$H_\delta' \in [-0.00625, 0.00625]$

:
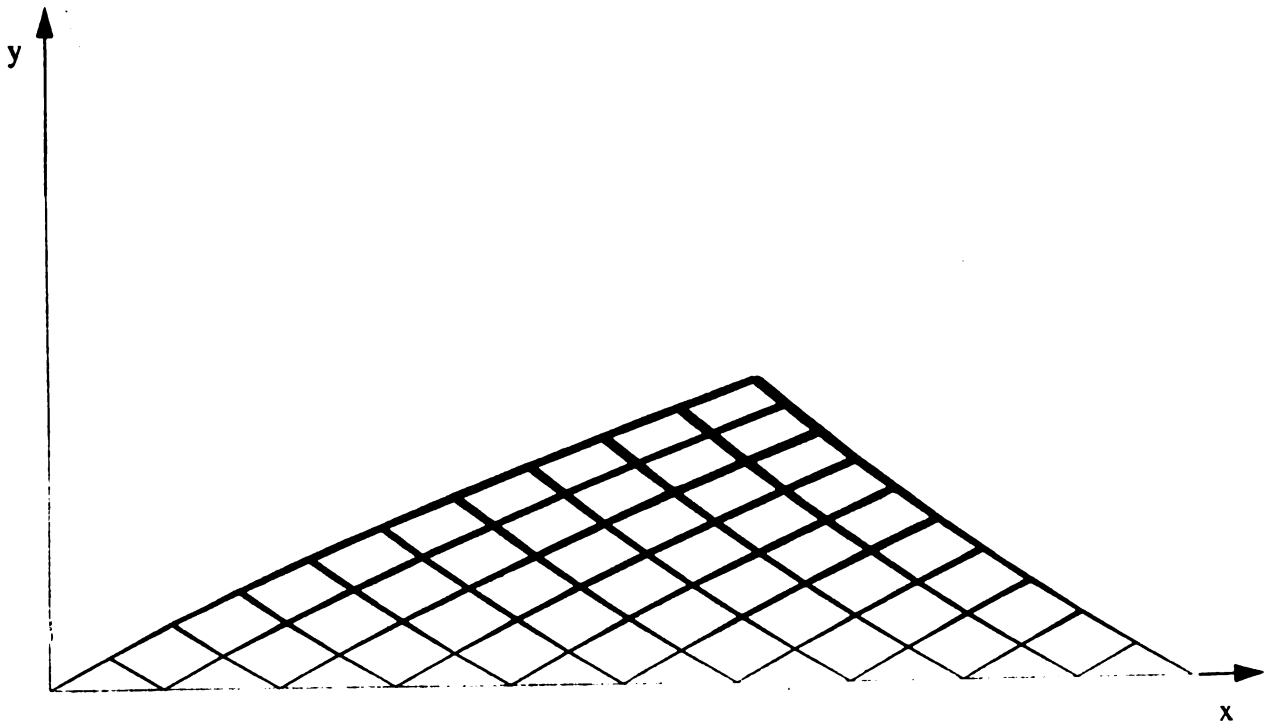
Fig. 3.4 The inhomogenous solution of the Cauchy boundary value
problem from Sokolovskii, 1965. ch 1. pp49

3.5 The Characteristic Boundary Value Problem.

The characteristic boundary value problem was investigated for the case of a granular medium in more detail in Section 3.8, and is defined as one in which the values of the function p and of the angle φ are given along the characteristics AB and AC belonging to two different families of characteristics. Henceforth, $y_\alpha(x)$ stands for AB and $y_\beta(x)$ stands for AC.
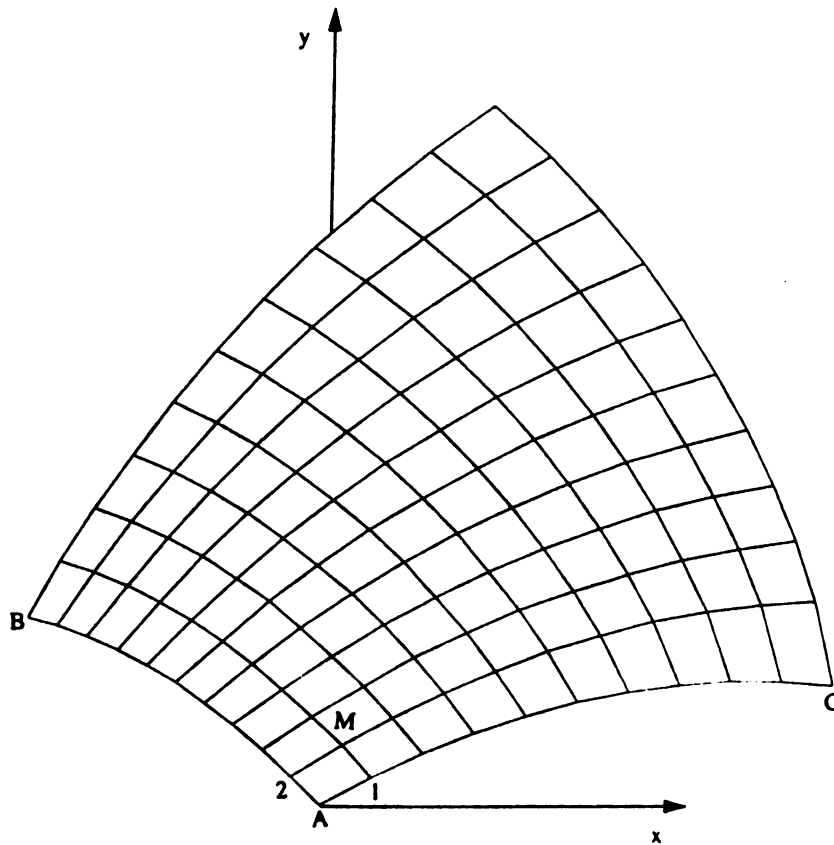
Fig 3.5 Characteristic boundary value problem

The angle φ is determined by the direction of the characteristic, namely:

$$\varphi_{AC} = \text{atan}\left(\frac{dy_\beta}{dx}\right) - \varepsilon \qquad (3.62)$$

$$\varphi_{AB} = \text{atan}\left(\frac{dy_\alpha}{dx}\right) + \varepsilon \qquad (3.63)$$

The values of function σ along each of the two families of characteristics are found immediately if σ is given at a single point, not necessarily point A. Relations (3.16):

$$\sigma \cdot e^{\mp 2 \tan(\rho)\varphi} = \text{constant} \qquad (3.64)$$

hold along α and β characteristics respectively and allow to determine σ within the domain of influence. The numerical procedure is the same as in the case of a Cauchy boundary value problem. Partitioning both curves in n segments, one can find the values of σ and φ at every point on the boundary. Starting from points 1 and 2 which are in the immediate vicinity of point A, using the same sequence of calculations as in the case of a Cauchy problem, one can find the values of σ_M and φ_M at the new point M as well as its coordinates x_M and y_M. Having found the magnitudes of all the points M on a row, or column, we can march forward and find the solution in the whole domain of influence, therefore the stresses may be found.

3.6 The Characteristic Boundary Value Problem with a Singular Point.

This problem is a very important particular case of the Characteristic Boundary

Value Problem since it occurs in most plasticity problems of a certain difficulty. The problem can be obtained from the previous one when one shrinks one of the characteristics, i.e. its length tends to zero whereas the increment in the angle φ on that segment has a finite value, $\Delta\varphi$:

a)   b)
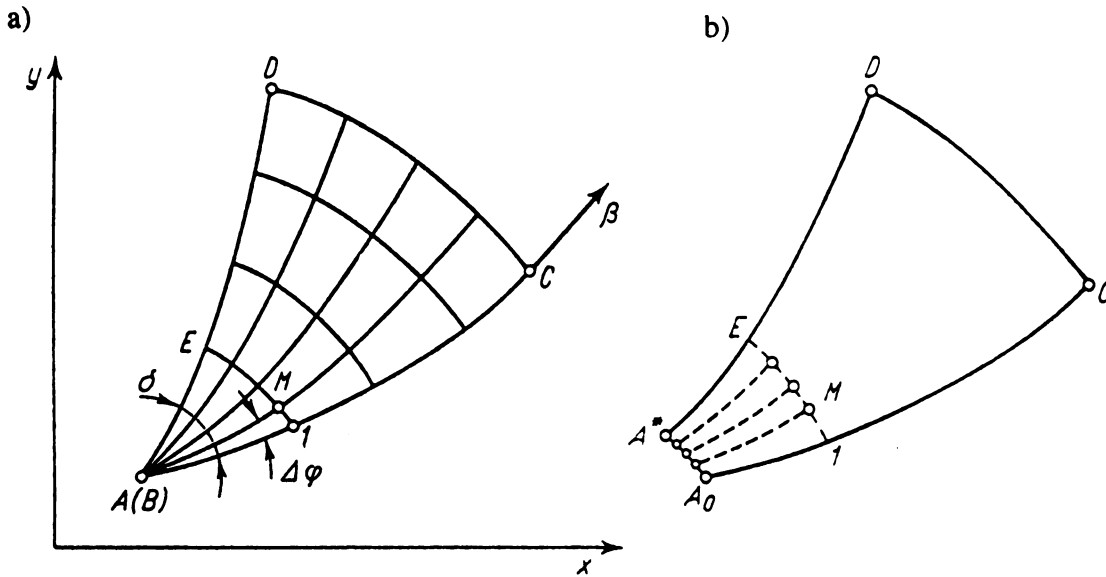
Fig 3.6 Characteristic boundary value problem with singular point
from [Szczepinski, 1979]

The total increment $\Delta\varphi$ must be first divided into a number of small increments corresponding to each of the points on the segment AB, shrunk into a single point, A:

$\delta\varphi = \dfrac{\Delta\varphi}{n}$. To show how the numerical procedure works, we will imagine that at A there are a number of overlapped points, from A_0 to A_n (Fig. 3.6 b). All of them possess the same coordinates, but the value of the angle φ increases by $\delta\varphi$ from one point to the other: at A_0 $\varphi_{A_0} = \varphi_A$ and at the ith point we have $\varphi_{A_i} = \varphi_A + (i - 1) \cdot \delta\varphi$. Using the same procedure as described above, one can find values of all the variables within the domain ACB.

3.7 The Mixed Boundary Value Problem.

In the following we will discuss just one of several boundary value problems which exist. More details can be found in [Szczepinski, 1979, Chakrabarty, 1987].

In a mixed BVP values are given along a characteristic line and moreover along a non-characteristic one. Let the segment AC be the characteristic, along which the values of σ and φ are known. Along AB of equation $y=y(x)$ that is known, the angle φ is known. These data are sufficient in order to find determine the problem in the whole region ABC. Excepting the points lying on the segment AB, similar numerical calculations have to be performed.
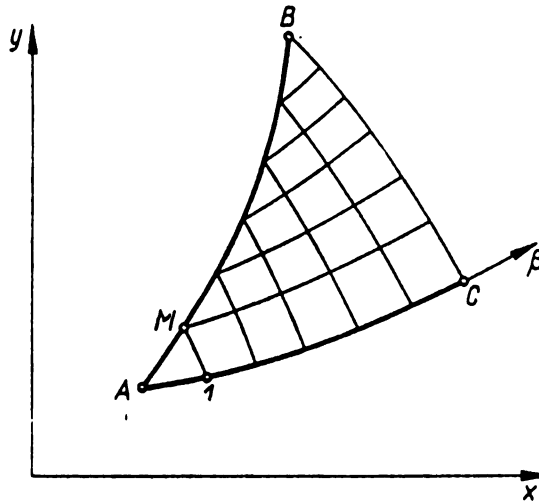
Fig. 3.7 Mixed boundary value problem
from [Szczepinski, 1979]

Let AC belong to the first family of characteristics. The coordinates x_M and y_M of the point M, at which the characteristic of the second family through the point 1 intersects AB, can be obtained from:

$$y_M - y_1 = \frac{1}{2} [\tan(\varphi_1 - \varepsilon) + \tan(\varphi_M - \varepsilon)] (x_M - x_1) \qquad (3.65)$$

and

$$y_M = y(x_M) \qquad (3.66)$$

of the line AB. The angle φ_M is known, therefore σ_M can be found using (3.52). In the same way one can solve the case when AC is a characteristic that belongs to the second family.

3.8 Discussion of Results.

In the present study the initial gradients of $y_\beta(x)$ and $y_\alpha(x)$ are 30° and $(-30+2\varepsilon)^\circ$ respectively, where ε is given by formula (3.20), at the origin of an xOy-coordinate system. In order to study the effects of homogeneous versus inhomogeneous boundary data, this boundary value problem is studied here in four cases covering various combinations of $y_\alpha(x)$ and $y_\beta(x)$ being either straight lines or second-order polynomials with negative curvature. Thus, we set up four different boundary value problems:

Problem #1:

$$y_\alpha = x \tan(-30^\circ + 2\varepsilon) \qquad y_\beta = x \tan(30^\circ) \qquad (3.67)$$

Problem #2:

$$y_\alpha = x \tan(-30° + 2\varepsilon) - \frac{x^2}{15} \qquad y_\beta = x \tan(30°) \qquad\qquad (3.68)$$

Problem #3:

$$y_\alpha = x \tan(-30° + 2\varepsilon) \qquad y_\beta = x \tan(30°) - \frac{x^2}{30} \qquad\qquad (3.69)$$

Problem #4:

$$y_\alpha = x \tan(-30° + 2\varepsilon) - \frac{x^2}{15} \qquad y_\beta = x \tan(30°) - \frac{x^2}{30} \qquad\qquad (3.70)$$

In all the above we take $x(i) = (i - 1) \cdot \dfrac{x_{max} - x_{min}}{n - 1}$ for $i = 0, 1, ..., n$.

Each one of these figures was obtained from 200 simulation runs, using exactly the same sequence of random numbers and employing forward differencing. The angle ρ and the ultimate resistance to the uniform three dimensional tension H -see figure 3.8, were taken to be:

$$\langle \rho_\delta(\omega) \rangle = 15°, \qquad H_\delta(\omega) = \frac{H_{0\delta}(\omega)}{\tan(\rho_\delta(\omega))}, \qquad \langle H_{0\delta}(\omega) \rangle = 0.6 \qquad\qquad (3.71)$$
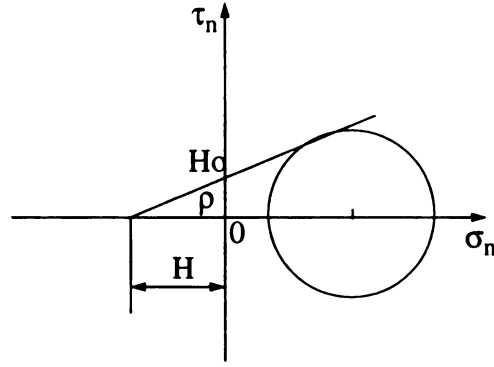
Fig 3.8 The Mohr stress diagram

Numerical results of simulation of Problem #1, in three cases of randomness:

$$\rho' \in [-0.015, 0.015], \ H_0' \in [-0.0006, 0.0006] \tag{3.72}$$

$$\rho' \in [-0.025, 0.025], \ H_0' \in [-0.001, 0.001] \tag{3.73}$$

$$\rho' \in [-0.075, 0.075], \ H_0' \in [-0.003, 0.003] \tag{3.74}$$

are shown in the sequence a), b) and c) of Fig. 3.9, while those of Problem #2 in the sequence d), e) and f) of this figure. For computational reasons, we considered H_0 to be the random variable instead of H, the relationship between these two being given by (3.71).

One notes here a gradual sensitivity of the slip-line nets to material randomness and to the inhomogeneity in the boundary data. This latter type of sensitivity is confirmed by Fig. 3.10, which gives solutions to Problem #3 - a), b) and c) - and to Problem #4 - d), e) and f) - also in three cases of randomness given by (3.72), (3.73), and (3.74)

a) Problem #1, noise x
according to (3.72)

d) Problem #2, noise x
according to (3.72)

b) Problem #1, noise x
according to (3.73).

e) Problem #2, noise x
according to (3.73).

c) Problem #1, noise x
according to (3.74).

f) Problem #2, noise x
according to (3.74).

Fig. 3.9 Characteristic boundary value problems

a) Problem #3, noise according to (3.72)

b) Problem #3, noise according to (3.73).

c) Problem #3, noise according to (3.74).

d) Problem #4, noise according to (3.72)

e) Problem #4, noise according to (3.73).

f) Problem #4, noise according to (3.74).
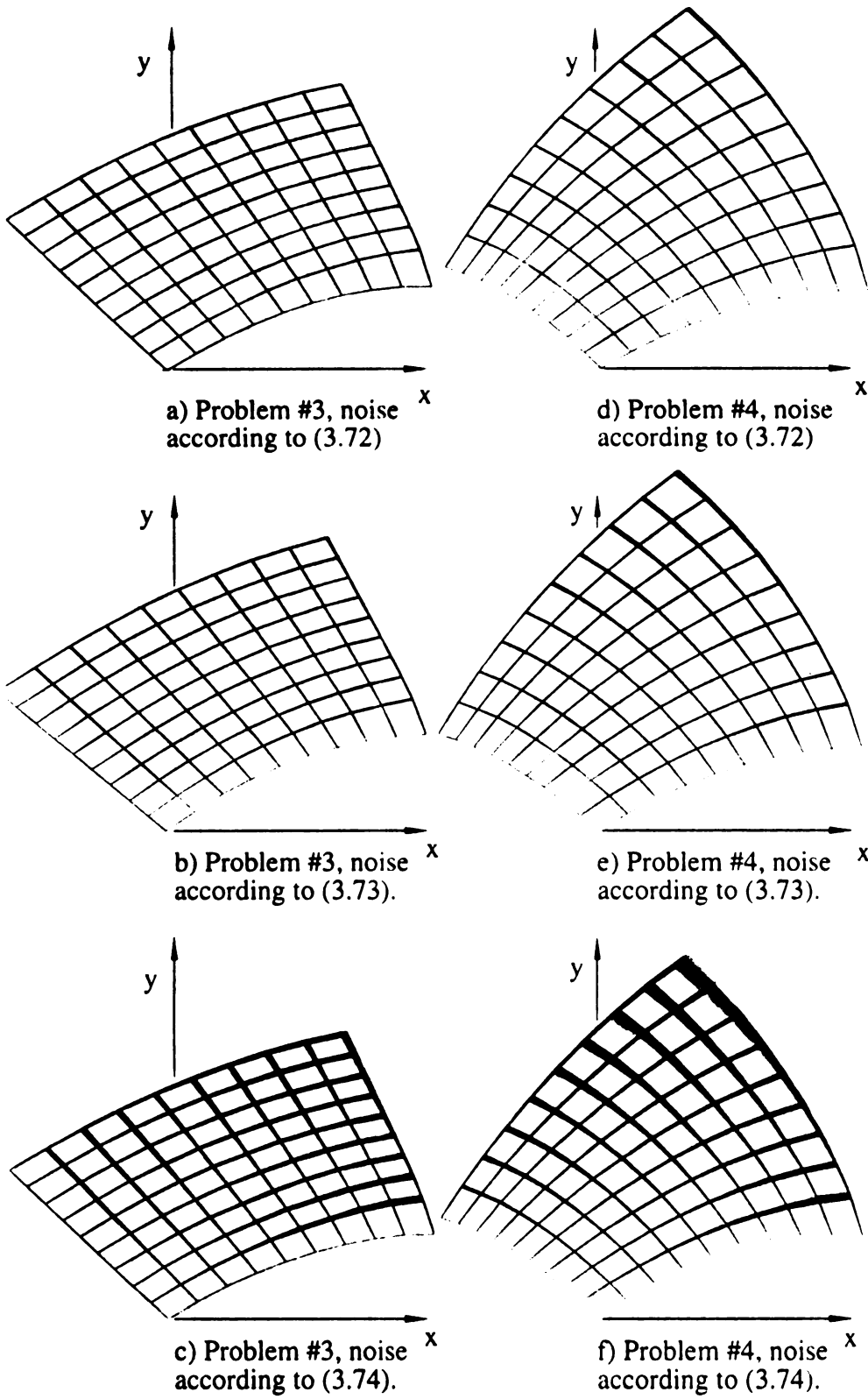
Fig. 3.10 Characteristic boundary value problems

We investigated for the characteristic boundary value problem of an inhomogeneous granular medium - illustrated in fig 3.10 f) - the probability distribution of the maximum distance from the origin and of the three stresses, i.e. σ_x, σ_y and τ_{xy} at that point. It was observed that, even though for the maximum polar radius, the average solution of the random problem does not differ substantially from the deterministic BVP as can be seen in Fig. 3.11 a), the stresses have an average solution of the inhomogeneous problem always smaller compared to the one of the homogeneous medium, see Fig. 3.11 b) and Fig 3.12 a) and b) respectively. So we do need more material, but the stresses predicted by this theory are smaller, in average, than those predicted by the classical one. In figures 3.10 and 3.11 the variables ρ and H_0 were taken to be:

$$\langle \rho_\delta(\omega) \rangle = 15°, \qquad H_\delta(\omega) = \frac{H_{0\delta}(\omega)}{\tan(\rho_\delta(\omega))}, \qquad \langle H_{0\delta}(\omega) \rangle = 0.6$$

and the noise was according to (3.74)
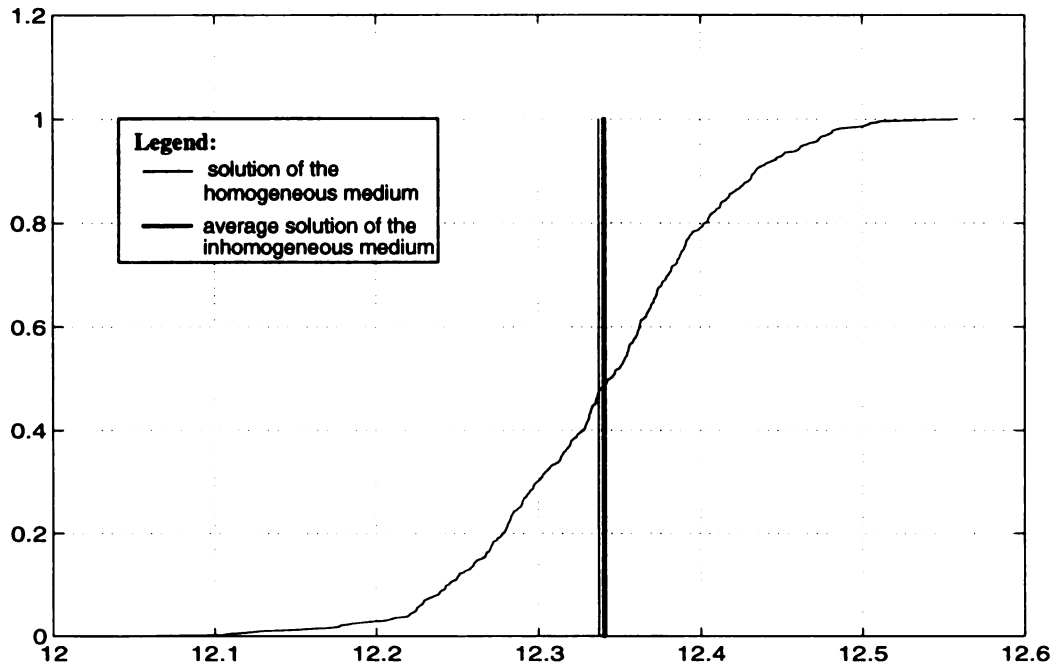
a) of the polar radius r(ω)
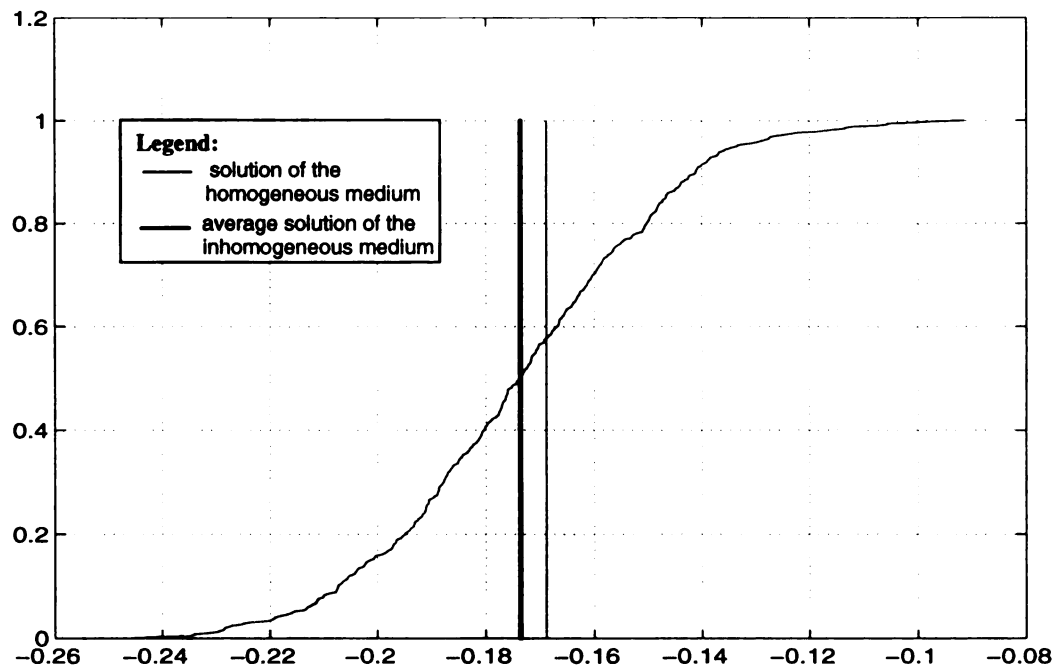
b) of the stress $\sigma_x(\omega)$

Fig. 3.11 The probability distribution at the corner point
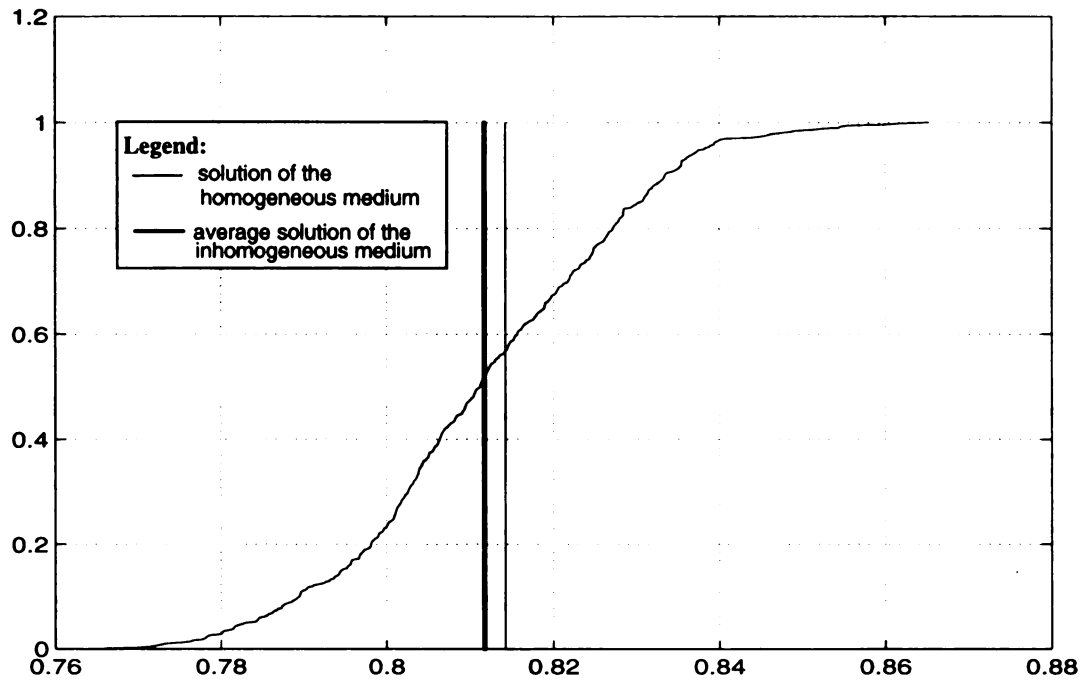
a) of the stress $\sigma_y(\omega)$
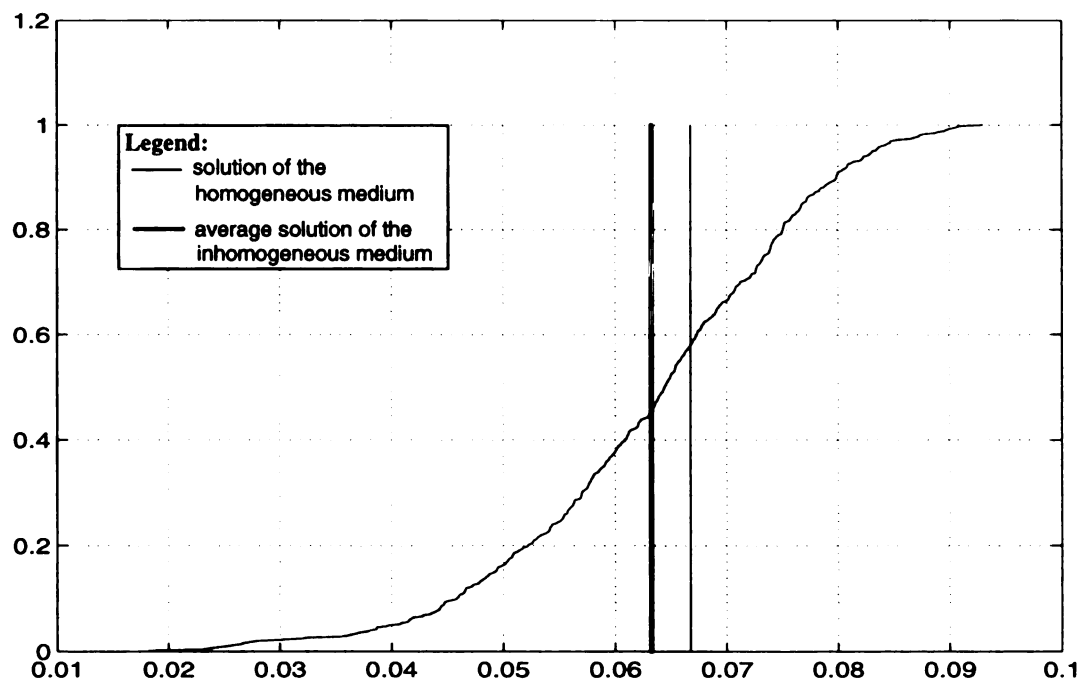
b) of the stress $\tau_{xy}(\omega)$

Fig. 3.12 The probability distribution at the corner point

In figure 3.13 we make a comparison of the same boundary value problem for two different media: one governed by the HMH criterion - a), the other by the MC criterion - b). In both cases, the β-characteristic is the same and specified by:

$$y_\beta = x - \frac{x^2}{10} \tag{3.75}$$

whereby the α-characteristic is given by the yield condition used. In both cases the noise is 5% about the mean, that is:

$$k_\delta' \in [-0.025, 0.025] \,, \quad \langle k_\delta \rangle = 0.6 \tag{3.76}$$

for the first case, where k_δ is a uniform random variable. For the second case (Fig. 3.13 b)):

$$\rho_\delta' \in [-0.375, 0.375] \qquad H_{0\delta}' \in [-0.015, 0.015] \tag{3.77}$$

where $\langle \rho_\delta \rangle = 15^\circ$, $\langle H_{0\delta} \rangle = 0.6$ and ρ_δ and $H_{0\delta}$ are both independent uniform random variables. The relatively stronger sensitivity of the MC-type material versus the HMH-type material, accompanied by a departure from the orthogonality of the slip-line net, is a typical feature here.
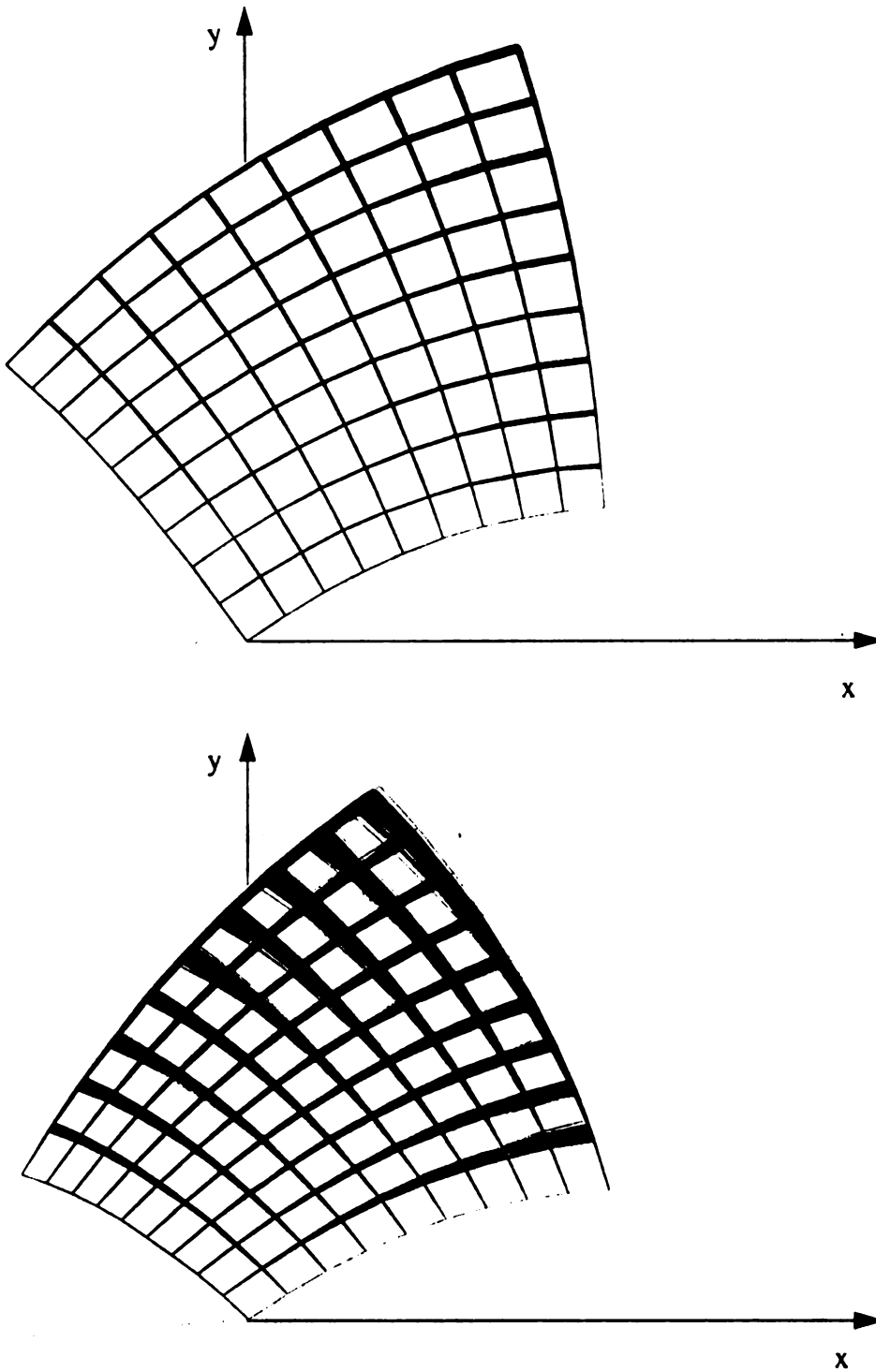
Fig. 3.13 The characteristic boundary value problem for materials of
(a) HMH-type, and (b) MC-type.

Based on the assumption that the internal friction coefficient, $\mu = \tan(\rho)$, is a random variable, a probabilistic failure criterion was developed in [Alpa and Gambarotta, 1990] where the Peano-Jordan derivative of the probability of failure as a function of the resolved tractions was assumed to have a Weibull form. There, the main conclusion was that the stresses given by the probabilistic criterion fit better the experimental data than those given by the deterministic MC yield criterion.

To better understand the effects of the randomness in ρ_δ and $H_{0\delta}$ on the response of an MC-type medium, we plot in Fig. 3.14 the mean of $r_\delta(\omega)$, its difference with respect to the deterministic medium $B_{det} = B(\rho_{det}, H_{det})$, and the standard deviation of the position $r_\delta(\omega)$ of the extremum point with respect to the origin. Figures. 3.15, 3.16 and 3.17 present the corresponding specifications for the stress components $\sigma_x(\omega)$, $\sigma_y(\omega)$ and $\tau_{xy}(\omega)$ at the same point. These graphs correspond to the characteristic boundary value problem shown in Fig. 3.13 b). The sequences a), b), c) of figures 3.14-3.17 correspond to uniform random variates while d), e), f), of the same figures, to Weibull type random variates. For sequences a), b) c) each point on the surfaces was obtained from 200 simulation runs, i.e. 200 different realizations of $B(\omega)$, while for d), e), f) 40 simulation runs were used for each particular point, due to computational reasons: in order to generate the Weibull type random variates we used the von Neumann acceptance-rejection method. For a single realization there are needed 200 random variates and for each of these numbers there are needed, in average, approximately 41 000 do loops of the random number generator, therefore we encountered some problems with the data storage. However, for 40 realizations the problem is stabilized.
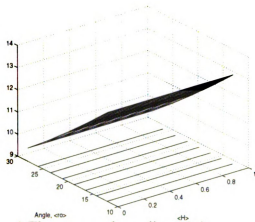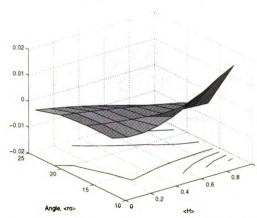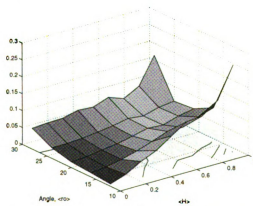
a) The mean polar radius, r(ω)
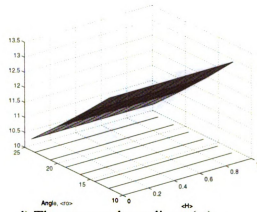
d) The mean polar radius, r(ω)
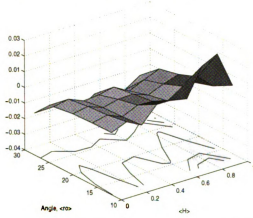
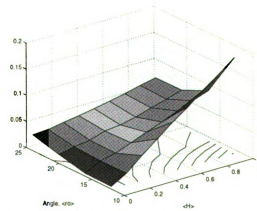

b) Its difference from the homogeneous medium
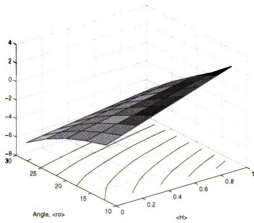

e) Its difference from the homogeneous medium
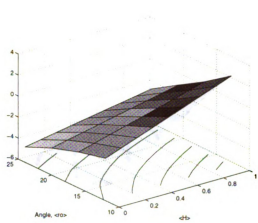

c) The standard deviation, STD(r(ω))

f) The standard deviation STD(r(ω))

Fig. 3.14 Statistical specifications of the polar radius
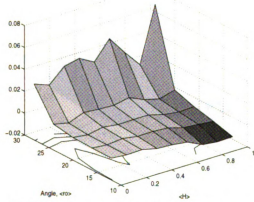a), b), c)- uniform type noise; d) e), f)- Weibull type noise

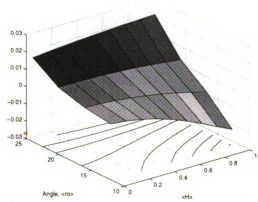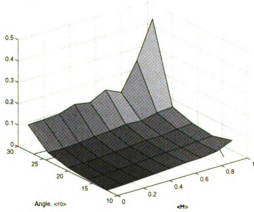a) The mean of the field variable $\sigma_x(\omega)$
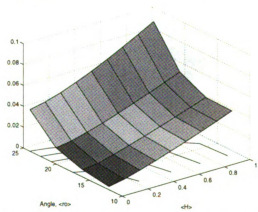

d) The mean of the field variable $\sigma_x(\omega)$

b) Its difference from the homogeneous medium

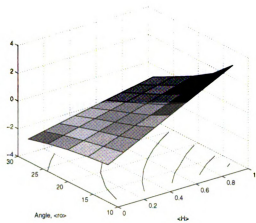e) Its difference from the homogeneous medium

c) The standard deviation, STD($\sigma_x(\omega)$)
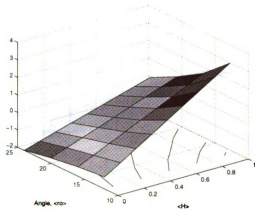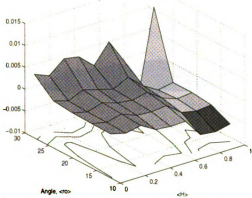

f) The standard deviation, STD($\sigma_x(\omega)$)

Fig 3.15 Statistical specifications of the field variable $\sigma_x(\omega)$
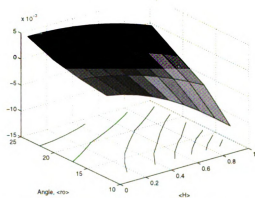a), b), c)- uniform type noise; d) e), f)- Weibull type noise

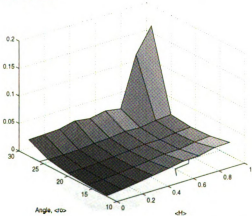a) The mean of the field variable $\sigma_y(\omega)$
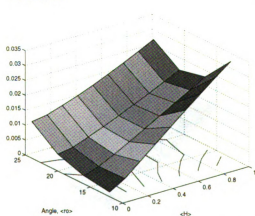

d) The mean of the field variable $\sigma_y(\omega)$

b) Its difference from the homogeneous medium

e) Its difference from the homogeneous medium

c) The standard deviation, STD($\sigma_y(\omega)$)

f) The standard deviation, STD($\sigma_y(\omega)$)

Fig. 3.16 Statistical specifications of the field variable $\sigma_y(\omega)$
a), b), c)- uniform type noise; d) e), f)- Weibull type noise

a) The mean of the field variable $\tau_{xy}(\omega)$

d) The mean of the field variable $\tau_{xy}(\omega)$

b) Its difference from the homogeneous medium

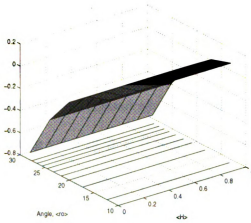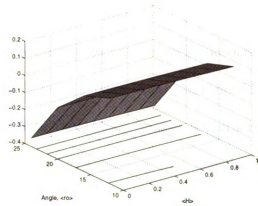e) Its difference from the homogeneous medium

c) The standard deviation, STD($\tau_{xy}(\omega)$)

f) The standard deviation, STD($\tau_{xy}(\omega)$)

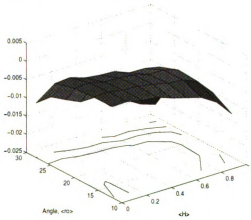Fig. 3.17 Statistical specifications of the field variable $\tau_{xy}(\omega)$
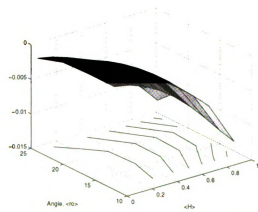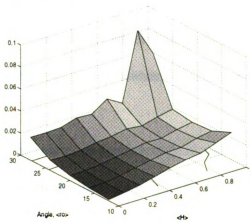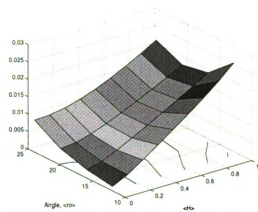a), b), c)- uniform type noise; d) e), f)- Weibull type noise

For both uniform and Weibull types of noises, standard deviations of all four dependent field variables have an increasing tendency with the increase in H_0. However, with increasing angle ρ, these standard deviations decrease and go to a minimum in the vicinity of 15 degrees, beyond which they start to increase. This is an interesting observation. The limiting value of $\rho = 0$ that corresponds to the Huber-von Mises-Henky yield criterion could not be obtained by running the program for the MC-type material. Note here that the variables ρ and H_0 have bounded domains due to the instability of the inhomogeneous problem at small values of angle ρ and relatively big values of H_0. On one hand, the expectations of r and τ_{xy} have a very small or no dependence upon H_0, as can be seen in Figs 3.14-3.17; on the other, the means of the two stresses σ_x and σ_y increase continuously with the increase in H_0; by increasing ρ the means of all four variables decrease. Moreover, the means of $r(\omega)$ and $\tau_{xy}(\omega)$ are approximately linear and quadratic in ρ. It is doubtful that the above results could be obtained analytically, in view of the nonlinear and stochastic nature of the problem.

A study of all the boundary value problems for a granular medium leads to the following principal conclusions regarding the effect of noises ρ_δ' and $H_{0\delta}'$:

i) The scatter in dependent field variables increases continuously with decreasing angle ρ and with the increase in the ultimate resistance to uniform three dimensional tension, H. However, ρ and H must be confined to certain finite ranges, dependent upon a particular noise level, in order for the problem to remain stable.

ii) Parameter ρ has a stronger influence than H; the limiting case of $\rho = 0$ could not be achieved with the MC-medium program, due to the instability of the inhomogeneous problem. However, as H tends to 0, i.e towards the cohesionless medium $H = 0$, the problem is still in the stable range.

iii) The average of the inhomogeneous stress distribution is always smaller than the deterministic one, and the difference increases with the noise and inhomogeneity of the boundary data.

iv) The standard deviations of the polar radius, $r(\omega)$ and stresses $\sigma_x(\omega)$, $\sigma_y(\omega)$ and $\tau_{xy}(\omega)$, of an MC-type of material, present a minimum in the interval $\rho = 15° \pm 3°$, which means that the characteristic boundary value problem is most stable in that interval.

v) Although in case of Weibull type noise the position and the field variables have smoother variations, the tendencies of variation do not change compared to those corresponding to uniform type noise. Moreover, in the latter case, the standard deviations are greater, which suggests that the characteristic BVP is less sensitive to Weibull type noise than to uniform type noise.

vi) The slip-line net of a granular material is dependent upon the integration method. Formula (2.24) recommended by [Szczepinski, 1979] stabilizes the problem while the others, e.g. (2.23) recommended by [Hill, 1950], do not; here, the explicit formulas were used first as a 'predictor' and then, without any convergence problems, the implicit formulas were

employed as a 'corrector'.

vii) For values of noise above 5% there is an increasing change in the average, and very amplified scatter, in the random fields of stress as well as position.

vii) The changes due to the Weibull type noise are more quantitative than qualitative. However, for this type of noise, the graphs showing the difference from the homogeneous medium and the standard deviations respectively are smoother. Moreover, in this case the standard deviations are smaller than in the case of uniform type noise, which suggests that the random rigid perfectly plastic medium is less sensitive to Weibull type variates than to uniform ones.

Thus we conclude that, in case of very small noise (e.g. given by (3.72)), one may replace the average solution of a stochastic problem by the solution of a deterministic problem with $\rho_{eff} = \rho_{det} = \langle \rho_\delta \rangle$ as well as $H_{eff} = H_{det} = \langle H_\delta \rangle$; that is $B_{eff} = B_{det}$. Given the fact that the governing system is a nonlinear stochastic one, this is an interesting observation.

All results in this chapter were obtained under the assumption of independence of random variables ρ_δ, $H_{0\delta}$ (i.e. H_δ as well) at all the points of the finite difference nets.

4. CONCLUSIONS

A major motivation for the research presented in this thesis has been the observation that the slip-line patterns observed in experiments on metals ([Kachanov, 1971] and [Mellor and Johnson, 1985]) differ from those predicted by classical deterministic medium theory. Similar discrepancies have been observed in soil mechanics ([Alpa and Gambarotta, 1990]). Our method allows an assessment of such differences through the determination of the statistics of slip-lines and stress fields. As mentioned in the Introduction, plasticity of random inhomogeneous media has recently been studied by Nordgren [1992] with a focus on stochastic theorems on limit load coefficients and an application to the loading of a wedge. Solution of this latter problem has been based on finding the mean of the minimum energy dissipation on the multiple branches of possible zig-zag velocity paths along the rigid-plastic boundary. This methodology differs from ours: we propose solving a given stochastic boundary value problem directly by calculating a large number (two hundred, say) of responses in a Monte Carlo sense. Given the power of today's computers, this is done in a couple of minutes, unless the mesh resolution is more than about fifty points, and yields practically the whole range of possible behaviors - that is, the probability distributions of slip-line fields and stress fields. This is in contrast to [Nordgren, 1992] which reports a need for extensive computational tasks.

Regarding the effect of random variates $\langle k'_\delta \rangle$ (HMH-type media) or ρ_δ' and $H_{0\delta}'$ (MC-type media) respectively, the following major conclusions can be drawn:

i) There is practically small difference between the ensemble average net of slip-lines of the stochastic problem (i.e. for a random medium B) and the net of a corresponding deterministic problem (i.e. for a homogeneous medium B_{det}) for very small noise (e.g. given by (3.72)); however, this difference increases with the growing inhomogeneity in the boundary data.

ii) The slip-line net of media governed by HMH yield criterion (i.e. metals) is independent upon the integration method, while is not true with MC-type media; for these types of media formula (2.24) recommended by [Szczepinski, 1979] stabilizes the problem while the others, e.g. (2.23) recommended by [Hill, 1950], do not.

iii) The choice of the forward (as used here) versus backward differencing scheme has only a small effect on the solution.

iv) More material is needed to withstand a given load than according to the classical theory. Inhomogeneities in the boundary data have a strongly amplifying effect on the scatter of dependent field quantities; for noise growing above 5% there is an increasing change in the average, and very amplified scatter, in the dependent field variables.

v) The granular medium governed by a Mohr-Coulomb yield criterion is more sensitive to noise than the Huber-Mises-Henky type medium (recall Fig. 3.13).

We conclude that in case of very small noise one may replace the average solution

of a stochastic problem by the solution of a deterministic problem with average properties, that is $B_{eff} = B_{det}$.

It should be mentioned here that this method can be applied to the determination of the velocity fields and can be extended to the hardening behavior and anisotropic yield conditions. Indeed, anisotropic yield conditions of a random character are expected from a micromechanical derivation; the subject remains a challenge for future research

Finally, it is of interest to mention that the present study has relations to another topic: transient stress waves in randomly linear and non-linear inhomogeneous media [Ostoja-Starzewski, 1991]. Mathematically these both problems are governed by stochastic quasi-linear hyperbolic systems. They both display Markov properties and share the concepts of forward evolution cones in place of unique characteristics of deterministic homogeneous media problems. However, the major difference between them lies in that the spacing of characteristics in a plasticity problem corresponds directly to a mesoscale, while no such mesoscale concept appears in the wavefront studies.

BIBLIOGRAPHY

BIBLIOGRAPHY

Adler, R.J., 1981, "The Geometry of Random Fields", *John Wiley & Sons.*

Alpa, G. and Gambarotta, L., 1990, "Probabilistic Failure Criterion for Cohesionless Frictional Materials", *J. Mech. Phys. Solids* 38(4), 491-503.

Hill, R., 1950, "The Mathematical Theory of Plasticity", *Oxford University Press, London.*

Chakrabarty, J., 1987, "Theory of Plasticity", *McGraw-Hill.*

Kachanov, L. M., 1971, "Foundations of the theory of plasticity", *North-Holland, Amsterdam.*

Nedderman, R. M., 1992, "Statics and kinematics of granular materials", *Cambridge University Press, Cambridge.*

Nordgren, R.P., 1992, "Limit Analysis of a Stochastically Inhomogeneous Plastic Medium with Application to Plane Contact Problems," *ASME J. Appl. Mech.* 59, 477-484.

Olszak, W., Rychlewski, J. and Urbanowski, W., 1962, "Plasticity under Inhomogeneous Conditions," *Adv. Appl. Mech.* 7, 132-214.

Ostoja-Starzewski, M., 1991, "Transient waves in a class of random heterogeneous media", *Appl. Mech. Rev.* (Special Issue: *Mechanics Pan-America 1991*) 44(10, Part 2), S199-S209.

Ostoja-Starzewski, M., 1992a, "Plastic Flow of Random Media: Micromechanics, Markov Property and Slip Lines", *Appl. Mech. Rev.,* Vol 45, No. 3, Part 2, pp S75-S81.

Ostoja-Starzewski, M., 1992b, "Boundary Value Problems in Plastic Flow of Random

Media", Symposium on Plastic Flow and Creep, *ASME Summer Mechanics and MAterials Conference,* Arizona State University; AMD-Vol. 135, MD-Vol. 31, pp 149-158.

Ostoja-Starzewski, M., 1993, "Micromechanics as a Basis of Stochastic finite elements and differences: An Overview", *Appl. Mech. Rev.,* Vol 46, No. 11, Part 2, pp S136-S147.

Ostoja-Starzewski, M., and Ilies, H., 1995, "The Cauchy And Characteristic Boundary Value Problems of Random Rigid-Perfectly Plastic Media", *International Journal of Solids and Structures,* in press.

Sanchez-Palencia, E., and Zaoui, A., 1987, "Homogenization Techniques for Composite Media", *Lecture Notes in Physics, Vol. 272, Springer-Verlag.*

Sokolowskii, V.V., 1965, "Statics of Granular Media", *Pergamon Press, Oxford.*

Szczepinski, W., 1979, "Introduction to the Mechanics of Plastic Forming of Metals", *Sijthoff&Noordhoff Int. Publ./PWN, Warsaw.*